



# Oxidative stress stimulates invasive potential in rat C6 and human U-87 MG glioblastoma cells via activation and cross-talk between PKM2, ENPP2 and APE1 enzymes

Ravi P. Cholia<sup>1</sup> · Monisha Dhiman<sup>2</sup> · Raj Kumar<sup>3</sup> · Anil K. Mantha<sup>1</sup>

Received: 18 December 2017 / Accepted: 6 April 2018  
© Springer Science+Business Media, LLC, part of Springer Nature 2018

## Abstract

Maintaining genomic integrity is essential for cell survival and viability. Reactive oxygen species (ROS) overproduction results in oxidative stress leading to the genomic instability via generation of small base lesions in DNA and these unrepaired DNA damages lead to various cellular consequences including cancer. Recent data support the concept “oxidative stress is an indispensable participant in fostering proliferation, survival, and migration” in various cancer cell types including glioblastoma cells. In this study we demonstrate that treatment of non-cytotoxic doses of oxidants such as amyloid beta [A $\beta$ (25–35)] peptide, glucose oxidase (GO), and hydrogen peroxide (H<sub>2</sub>O<sub>2</sub>) for 24 h and 48 h time points found to increase the expression level and activity of a multifunctional enzyme Apurinic/aprimidinic endonuclease (APE1), a key enzyme of base excision repair (BER) pathway which takes care of base damages; and also resulted in modulation in the expression levels of downstream BER-pathway enzymes viz. PARP-1, XRCC1, DNA pol $\beta$ , and ligase III $\alpha$  was observed upon oxidative stress in C6 and U-87 MG cells. Oxidants treatment to the C6 and U-87 MG cells also resulted in an elevation in the intracellular expression of glycolytic pathway enzyme Pyruvate kinase M2 (PKM2) and the metastasis inducer protein Ectonucleotide pyrophosphatase/phosphodiesterase 2 (ENPP2) as analyzed using Western blotting and Immunofluorescence microscopic studies. Our study also reports that oxidative stress induced for 24 h and 48 h in C6 and U-87 MG cells resulted in extracellular secretion of APE1 and ENPP2 as analyzed using Western blotting in conditioned media. However, the biological significance of extracellular secreted APE1 remains elusive. Oxidative stress also elevated the ENPP2's LysoPLD activity in conditioned media of C6 and U-87 MG cells. Our results also demonstrate that oxidative stress affects the expression level and localization of APE1, PKM2, and ENPP2 in C6 and U-87 MG cells. As evidenced by the colocalization pattern at 24 h and 48 h time points, it can be attributed that oxidative stress mediates crosstalk between APE1, PKM2, and ENPP2. In addition, when C6 and U-87 MG cells were treated with lysophosphatidic acid (LPA), a bioactive lipid that negatively regulates ENPP2's LysoPLD activity at 10  $\mu$ M concentration, demonstrated strong migratory potential in C6 and U-87 MG cells, and also induced migration upon oxidative stress. Altogether, the findings demonstrate the potential of C6 and U-87 MG cells to utilize three proteins viz. APE1, PKM2, and ENPP2 towards migration and survival of gliomas. Thus the knowledge on oxidative stress induced APE1's interaction with PKM2 and ENPP2 opens a new channel for the therapeutic target(s) for gliomas.

**Keywords** GBM · ROS · APE1 · PKM2 · ENPP2

✉ Anil K. Mantha  
anilmantha@gmail.com; anil.mantha@cup.edu.in

- <sup>1</sup> Department of Animal Sciences, School of Basic and Applied Sciences, Central University of Punjab, Bathinda, Punjab 151 001, India
- <sup>2</sup> Department of Biochemistry and Microbial Sciences, School of Basic and Applied Sciences, Central University of Punjab, Bathinda, Punjab, India
- <sup>3</sup> Department of Pharmaceutical Sciences and Natural Products, School of Basic and Applied Sciences, Central University of Punjab, Bathinda, Punjab, India

## Introduction

Tumor cells show modulated metabolic properties as they need more energy supply and also need more biosynthetic intermediates. Pyruvate kinase muscle isoform M2 (PKM2) is a key enzyme in the glycolytic pathway which catalyzes the terminal step of glycolysis, whose active tetrameric form converts phosphoenolpyruvate (PEP) into pyruvate (Mazurek 2011; Mazurek et al. 2005). Glioblastoma multiforme (GBM) is the most common primary brain tumor in adults

and aged individuals (Wrensch et al. 2002). GBM is aggressive in nature and shows elevated PKM2 expression in a grade-specific manner, but this does not correlate with pyruvate kinase activity. However, isoform switching between metabolic enzyme PKM1 and PKM2 has also been observed in GBM (Mukherjee et al. 2013). The ERK1/2-dependent PKM2 phosphorylation, PIN-1-dependent *cis-trans* isomerization and conversion of tetrameric PKM2 to monomeric form, subsequently resulting in its nuclear localization has been reported to be associated with cell cycle progression and tumorigenesis (Yang and Lu 2013). Lysophosphatidic acid (LPA) is a bioactive product of ectonucleotide pyrophosphatase/phosphodiesterase 2 (ENPP2) enzyme which dissociates PKM2 tetrameric form into dimeric form by causing metabolic inactivation of PKM2 (Desmaret et al. 2005).

Mantha et al. (2012) have identified PKM2's stable interaction with Apurinic/apyrimidinic endonuclease 1 (APE1) in PC-12 and SH-SY5Y cells upon A $\beta$ (25–35)-induced oxidative stress. APE1 is the major multifunctional enzyme which participates in the base excision repair (BER) pathway involved in the repairing of abasic (AP) sites in DNA, and also in the reductive activation of various cancer cell survival transcription factors (TFs) (Bhakat et al. 2009; Tell et al. 2010). Oxidative stress plays an important role in the elevation of APE1 activity in GBM which contributes to the resistance towards alkylating agents (Silber et al. 2002), and cancer cell survival by removing chemotherapy-induced DNA adducts in GBM (Johannessen and Bjerkvig 2012). Recently, we also demonstrated that oxidative stress accounts for modulation in antioxidant state, APE1 elevation and its nuclear localization in the glial cells (Cholia et al. 2017).

ENPP2 is a well-characterized second of seven members of the ectonucleotide pyrophosphatase/phosphodiesterase family, capable of hydrolyzing the phosphodiester or pyrophosphate bonds from a variety of substrates. ENPP2 is the only secreted protein from this family which also possesses lysophospholipase D activity (Hausmann et al. 2013). Elevated ENPP2 expression and LPA receptors are predominant in GBM, which plays a key role in its growth and development (Kishi et al. 2006). LPA signalling modulates the morphology of GBM cells (Fukushima et al. 2000) and enhances their invasive potential (Kishi et al. 2006).

The present study evaluates the oxidative stress responses induced in the rat and human glioma cells following treatment of oxidants [Hydrogen peroxide (H<sub>2</sub>O<sub>2</sub>), Glucose Oxidase (GO), and Amyloid beta (A $\beta$ ) peptide] to understand the aggressiveness displayed by the GBM. This study evaluates for the alteration in expression, activities, and cross-talk between

the enzymes APE1, PKM2, and ENPP2; which might be governing the underlined mechanisms contributing towards the GBM aggressiveness.

## Methodology

### Cell culture and treatments

Human glioma U-87 MG and rat glioma C6 cells (gifted by Prof. Gursharan Kaur, Guru Nanak Dev University, Amritsar, India) were maintained and cultured in DMEM media (Gibco) supplemented with 10% FBS (Gibco) and 1X penicillin-streptomycin solution (HiMedia) in humidified CO<sub>2</sub> incubator (Eppendorf) at 37 °C. For different treatments, C6 and U-87 MG cells were seeded in 96-well plates at a density of 1 × 10<sup>4</sup> cells per well or in 10 cm dishes at a density of 1 × 10<sup>6</sup> cells per plate. A $\beta$ (25–35) [Genscript], H<sub>2</sub>O<sub>2</sub> (MP-Biomedicals), and GO (Sigma) at various concentrations as indicated were used to induce the oxidative stress in the C6 and U-87 MG cells as suggested in various previously performed studies (Alía et al. 2006; Duthie et al. 1997; Cholia et al. 2017).

### MTT assay

C6 and U-87 MG cells survival was analyzed with MTT assay as described by Dhiman et al. (2012) with slight modifications in the protocol (Cholia et al. 2017). Cells were seeded (8000 cells/well) in 96-well plates and were incubated for 24 h at 37 °C. Cells were serum starved overnight and then treated with various concentrations of oxidants A $\beta$ (25–35) peptide (0–80  $\mu$ M), H<sub>2</sub>O<sub>2</sub> (0–200  $\mu$ M) and GO (0–100  $\mu$ U/ml) for 24 h and 48 h time points. Afterwards, 100  $\mu$ l of MTT (0.5 mg/ml) reagent (Invitrogen) was added to each well and incubated for 3 h in the dark at 37 °C. The purple colored formazan product was dissolved in acidified DMSO. O.D. was measured by using a microplate reader (Biotek) at 570 nm. A graph was plotted with percent relative cell viability on the y-axis against oxidant concentration on the x-axis.

### Intracellular ROS measurement

Intracellular ROS was measured using H<sub>2</sub>DCFDA reagent as described previously (Cholia et al. 2017). Approximately 8000 C6 and U-87 MG cells/well were seeded in 96 well plate. Cells were serum starved overnight, and oxidants (A $\beta$ (25–35) peptide, H<sub>2</sub>O<sub>2</sub> and GO) treatment was given to the cells for 24 h and 48 h time points. Afterward, cells were

incubated with 100  $\mu$ l of 50  $\mu$ M H<sub>2</sub>DCFDA (Thermo Fisher) solution for 30 min in the dark and washed with 1X phosphate buffered saline (PBS). A blank reading was recorded at excitation/emission 478/518 nm, and cells were further incubated for 30 min in the dark and the measurements were recorded. Relative fluorescence intensity was measured and the data represented as percent change in ROS.

### Western blot analysis

C6 and U-87 MG cells were lysed using RIPA buffer [20 mM Tris-HCl (pH 7.4), 150 mM NaCl, and 1 mM EDTA] supplemented with protease inhibitor cocktail (Amresco) as described previously with few modifications (Mantha et al. 2012). Protein samples (total cell lysate 30  $\mu$ g each or conditioned media 40  $\mu$ L each) were separated by electrophoresis on 8–10% SDS-PAGE and blotted onto PVDF membranes (Pall, Life Sciences). Then the membranes were blocked for 1 h in 5% non-fat dry milk (BioRad) in 50 mM Tris-HCl (pH 7.4), containing 0.05% Tween 20 (TBST). Blocked membranes were incubated with primary antibody for PCNA, APE1, PKM2, Autotaxin (Santa Cruz), and ENPP2 (Sigma) and then incubated with the secondary antibody (1:5000; Invitrogen).  $\beta$ -Actin (Santa Cruz) was used as endogenous control for normalization. The immune detection was accomplished using ECL reagent (BioRad), and protein expression were visualized using FluorChem HD2 (Protein Simple) gel documentation system.

### Immunocytochemistry

Cellular localization of APE1 was determined using immunocytochemistry staining as described (Singh and Englander 2012). A constant cell suspension was poured on sterile coverslips placed in each well and the U-87 MG and C6 cells were treated with oxidants for 24 h and 48 h. Following incubation, cells were fixed with 4% formaldehyde solution for 20 min and permeabilized using 0.1% Triton X-100 for 10 min. Cells were blocked using 10% FBS for 1 h at room temperature. Then the cells were washed and incubated at 4 °C overnight with primary APE1, PKM2 (1:100; Santa Cruz) and ENPP2 (1:100; Santa Cruz) antibodies. Cells were washed three times with 1X sterile PBS and incubated with secondary antibodies Alexa Fluor 488/568/647 (Invitrogen) for 1 h. Then the cells were washed three times with 1X sterile PBS and incubated with DAPI for 10 min for nuclear staining, and images were captured under the 60X oil objective using confocal laser scanning microscope (FV1200, Olympus) at the Central Instrumentation Laboratory (CIL), Central University of Punjab, Bathinda (CUPB).

### Wound healing assay

Approximately  $2 \times 10^5$  C6 and U-87 MG cells per well were seeded in 6-well plates and allowed to grow upto 70% confluency at 37 °C in a humidified, 5% CO<sub>2</sub> maintained incubator for 24 h. Media was replaced with serum-free media containing 0.1% fatty acid-free BSA (Sigma-Aldrich) to synchronize the cell growth. With a sterile 200  $\mu$ l pipette tip, a cell-free straight streak/wound was created. Cells were washed with 1X sterile PBS to remove any debris or floating cells. The cell division was arrested using mitomycin C (Sigma) treatment for 2 h before the oxidants treatment (Schleicher et al. 2011). Zero h image of cell-free streak/wound was taken at 10X objective lens using Olympus Magnus inverted microscope equipped with Sony Color Video Camera using TV Home Media2 software. The oxidants, A $\beta$ (25–35) peptide (10  $\mu$ M), GO (10  $\mu$ U) and H<sub>2</sub>O<sub>2</sub> (50  $\mu$ M) treatment with/without LPA (10  $\mu$ M; Sigma) was given to the C6 and U-87 MG cells and incubated for 24 h. After the incubation media was discarded and cells were washed with 1X sterile PBS and cells were fixed with methanol, followed by staining with 1% crystal violet. To quantify the wound healing, cells in 3 random scratch areas were selected and counted under the 10X objective lens. Wound healing was quantified by calculating the number of migratory cells in the streak area with a mean and standard error for each treatment group as described earlier with minor modifications (Schleicher et al. 2011). A graph was plotted of cells in wound area on the y-axis against oxidants treatment on the x-axis.

### Preparation of conditioned media

For the assessment of extracellular protein levels and activities, a conditioned media was prepared from approximately 80% confluent cultured U-87 MG and C6 cells (treated/non-treated). Cells were seeded at a constant number in 10 cm dishes for overnight growth following which the media was replaced with serum-free media containing 0.1% fatty acid-free BSA to synchronize the cell growth. Cells were treated with oxidants for 24 h and 48 h time points. Afterwards, the treatment incubation media was removed from the cells and clarified by centrifugation at 3000 rpm for 5 min at 4 °C to remove any cellular debris and dead cells. The supernatant was transferred to pre-cooled new sterile 15 ml tubes and filtered through 0.2  $\mu$ m filter as described previously (Wu et al. 2010). Filtered media was concentrated using concentrator (Millipore) as indicated in manufacturer's protocol. Concentrated conditioned media was supplemented with protease inhibitors and stored at –20 °C until further use.

## LysoPLD activity of ENPP2

LysoPLD activity of ENPP2 was measured using the N-ethyl-N-(2-hydroxy-3-sulfopropyl)-3-methylaniline (TOOS) activity assay as described earlier (Katsifa et al. 2015). ENPP2 catalyzes the cleavage of lysophosphatidylcholine (LPC) to LPA and choline. The released choline is oxidized by choline

oxidase to produce betaine and  $H_2O_2$ , which acts as an oxidizing agent. In the presence of horseradish peroxidase (HRP),  $H_2O_2$  reacts with TOOS and 4-AAP (amino antipyrine) to form a pink quinonimine dye which absorbs at 555 nm. Using 1X LysoPLD buffer [100 mM Tris-HCl (pH 9.0); 150 mM NaCl, 5 mM  $MgCl_2$ , 5 mM  $CaCl_2$ , 60  $\mu M$   $CoCl_2$ , and 1 mM LPC] at 37 °C for 30 min reaction was observed.

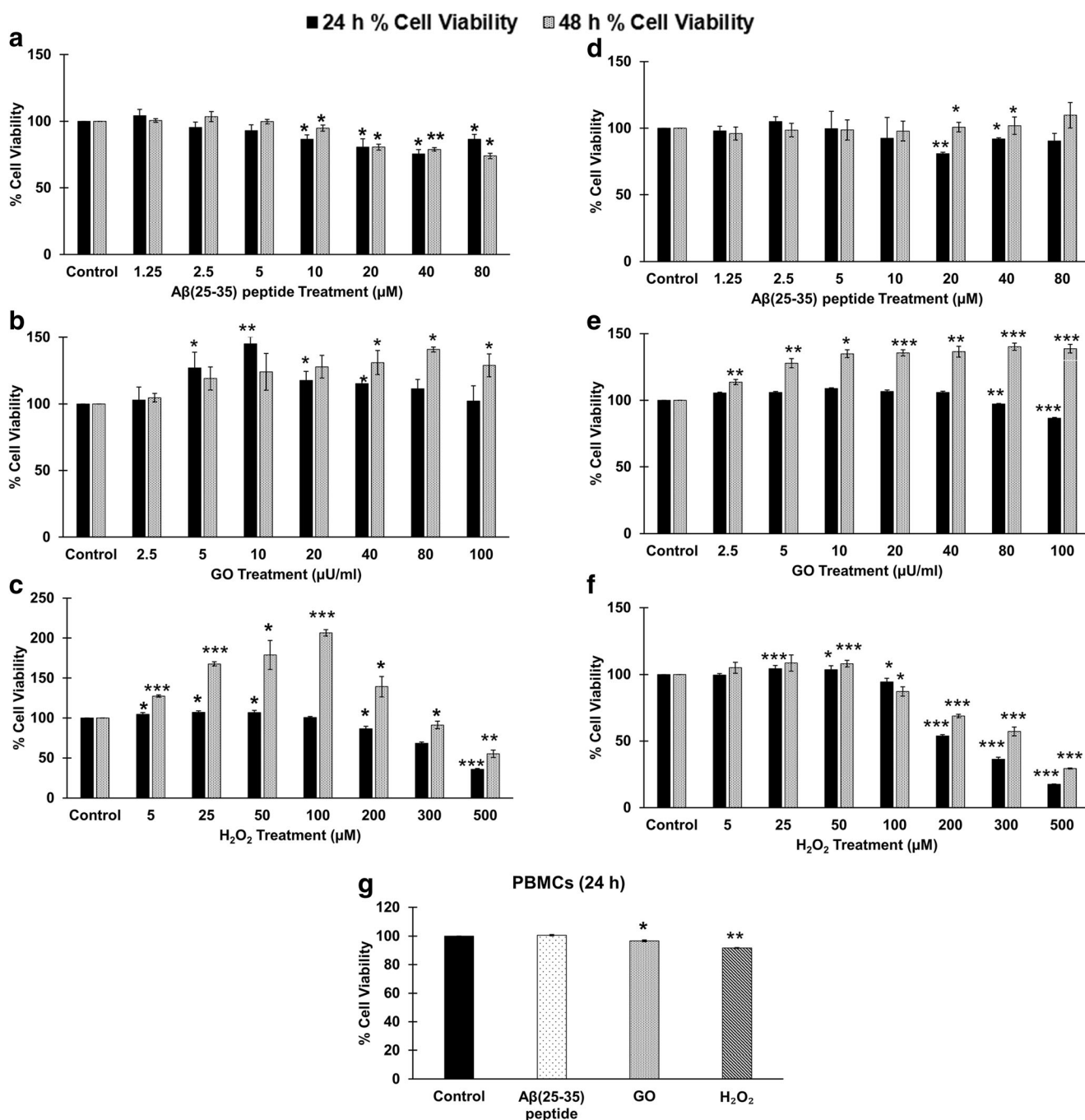


**Fig. 1** MTT assay showing the effect of varying dose of Aβ(25–35) peptide, GO, and  $H_2O_2$  on percent cell viability compared with that of untreated control cells for 24 h, and 48 h in C6 (**a**, **b**, & **c**); and in U-87 MG (**d**, **e**, & **f**). Effect of selected doses of Aβ(25–35) [10 μM], GO (10

μU/ml) and  $H_2O_2$  (50 μM) on cell viability of human peripheral blood mononuclear cells PBMCs for 24 h (**g**). The results are expressed as a mean ± standard deviation ( $n=3$ ). The data is considered as statistically significant at \* $p \leq 0.05$ , \*\* $p \leq 0.01$ , and \*\*\* $p \leq 0.001$

Concentrated media from oxidants treated cells (10  $\mu$ l) were incubated with 1X LysoPLD buffer at 37  $^{\circ}$ C for 4 h in a final volume of 100  $\mu$ l in a 96-well plate. At the end of the incubation, a color mix [0.5 mM 4-AAP, 7.95 U/ml HRP, 0.3 mM TOOS, 2 U/ml choline oxidase in 5 mM  $MgCl_2$ /50 mM Tris-HCl (pH 8.0)] was prepared, and 100  $\mu$ l was added to each well. Absorbance was measured at 555 nm every 5 min interval for 20 min duration. For each sample, the absorbance was

plotted against time, and the slope (dA/min) was calculated for the linear (steady-state) portion of each reaction.

**ENPP2 activity was calculated as:**

$$\begin{aligned} \text{Activity (U/ml)} &= (\mu\text{mol/min/ml}) \\ &= [\text{dA/min (sample)} - \text{dA/min (blank)}] \\ &\quad \times Vt / (e \times Vs \times 0.5) \end{aligned}$$

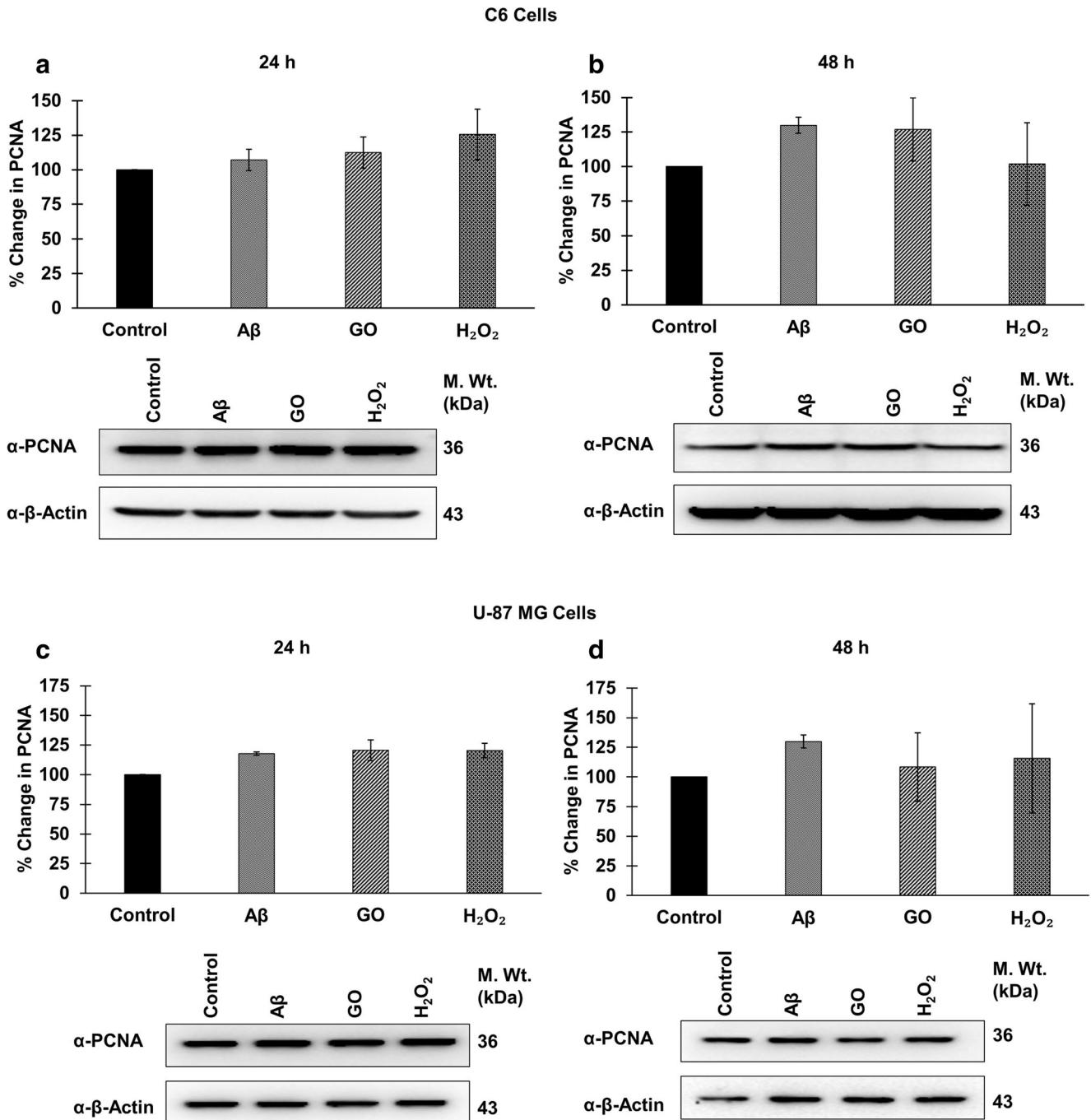


**Fig. 2** Western blot analysis of PCNA protein level in the total cell lysates of C6 cells (a & b) and U-87 MG cells (c & d) treated with oxidants [10  $\mu$ M A $\beta$ (25–35) peptide, 10  $\mu$ U/ml GO, and 50  $\mu$ M H<sub>2</sub>O<sub>2</sub>]. The results are expressed as a mean  $\pm$  standard deviation (n = 3)

Where,  $V_t$ : total volume of reaction (ml);  $V_s$ : volume of sample (ml);  $\epsilon$ : millimolar extinction coefficient of quinonimine dye under the assay conditions ( $\epsilon = 32.8 \mu\text{mol}/\text{cm}^2$ ); and 0.5: the moles of quinonimine dye produced by 1 mol of  $\text{H}_2\text{O}_2$ .

### Endonuclease activity of APE1

APE1's DNA repair activity was determined using gel based endonuclease assay. pUC19 plasmid DNA (gifted by Dr. Narottam Acharya, Institute of Life Sciences, Bhubaneswar, Odisha) was depurinated (*dp*) by incubating in 0.01 M sodium citrate, 0.1 M NaCl (pH 5.2) at 70 °C in hot water bath for 45 min to induce AP sites. The *dp* plasmid DNA was used as a substrate for APE1's endonuclease (repair) activity. The *dp* DNA was incubated with 50 mM HEPES-KOH (pH 7.5), 50 mM KCl, 100  $\mu\text{g}/\text{ml}$  BSA, 10 mM  $\text{MgCl}_2$ , 0.05% Triton X-100 at 37 °C for 10 min with nuclear extracts (NEs) of U-87 MG and C6 cells (treated or non-treated) to determine the repair activity of endogenous APE1. Then the reaction was stopped by adding 5  $\mu\text{l}$  electrophoresis sample buffer (1 mM EDTA, 0.25% bromophenol blue, 0.25% xylene cyanol and 50% glycerol) and incubated for 5 min at  $-20^\circ\text{C}$  and then analyzed using 0.7% agarose gel as described previously (Chen et al. 1991; Redaelli et al. 1998).

### Statistical analysis

Student's t-test was used to establish whether significance difference existed between the experimental groups. The

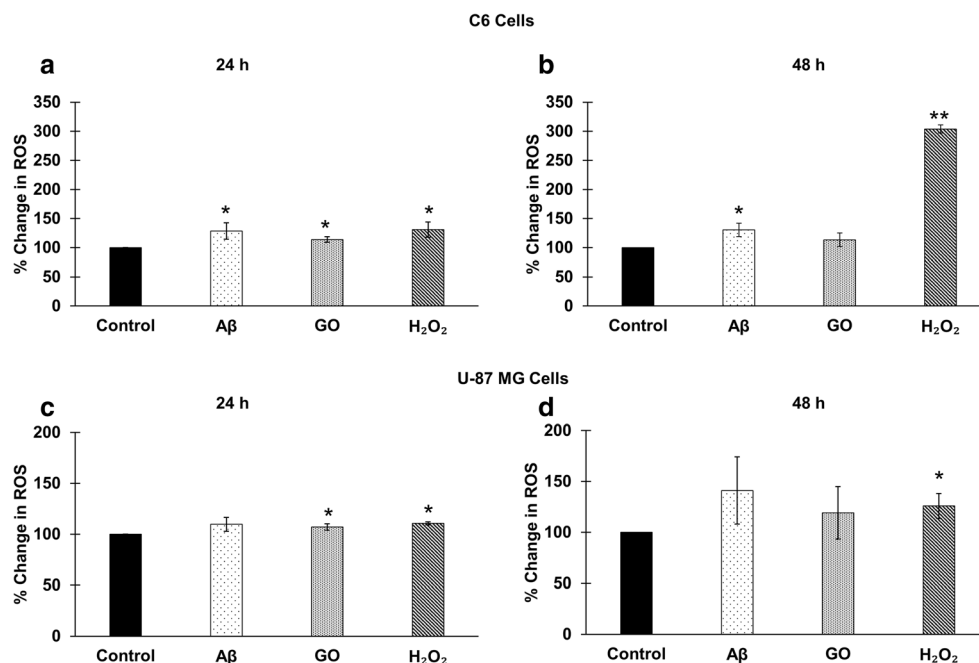
mean and standard deviation of each treatment group was calculated for all the experiments. The results are expressed as a mean  $\pm$  standard deviation ( $n = 3$ ). All  $p$ -values were of two-sided and the data considered statistically significant at  $*p \leq 0.05$ ,  $**p \leq 0.01$ , and  $***p \leq 0.001$  difference.

## Results

### Oxidants $\text{H}_2\text{O}_2$ , GO, and $\text{A}\beta(25-35)$ induces dose-dependent cytotoxicity in C6 and U-87 MG cells

U-87 MG and C6 cells were exposed to  $\text{H}_2\text{O}_2$  (0–500  $\mu\text{M}$ ), GO (0–100  $\mu\text{U}/\text{ml}$ ), and  $\text{A}\beta$  (0–80  $\mu\text{M}$ ) for 24 h and 48 h time periods.  $\text{A}\beta(25-35)$  peptide treated cells showed a decrease in the cell proliferation in a concentration-dependent manner in U-87 MG and C6 cell lines.  $\text{A}\beta(25-35)$  at 10  $\mu\text{M}$  displayed a non-cytotoxic effect. Dose dependent increase in cell proliferation was observed upto 20  $\mu\text{U}/\text{ml}$  GO treatment, and thereafter a constant increase in proliferation was observed upto 80  $\mu\text{U}/\text{ml}$ , as compared to the control C6 and U-87 MG cells after treatment for 24 h and 48 h time points. GO at 10  $\mu\text{U}/\text{ml}$  was effective to induce proliferation in C6 and U-87 MG cells without any cytotoxicity.  $\text{H}_2\text{O}_2$  treatment upto 100  $\mu\text{M}$  showed no cytotoxic effect in C6 and U-87 MG cells, whereas an increase in  $\text{H}_2\text{O}_2$  concentration beyond 100  $\mu\text{M}$  was found to be cytotoxic to the cells. From these results, 50  $\mu\text{M}$   $\text{H}_2\text{O}_2$  was found to induce the proliferation of C6 and U-87 MG cells at all the time points (Fig. 1a, b, c, d, e & f). Further, to confirm the non-

**Fig. 3** Percent change in ROS (Intracellular) using fluorescent  $\text{H}_2\text{DCFDA}$  assay in C6 (a & b) and U-87 MG (c & d) cells upon treatment with oxidants [10  $\mu\text{M}$   $\text{A}\beta(25-35)$  peptide, 10  $\mu\text{U}/\text{ml}$  GO, and 50  $\mu\text{M}$   $\text{H}_2\text{O}_2$ ]. The results are expressed as a mean  $\pm$  standard deviation ( $n = 3$ ). The data is considered as statistically significant at  $*p \leq 0.05$ , and  $**p \leq 0.01$



cytotoxic effect of the selected concentrations of oxidants, isolated human peripheral blood mononuclear cells (PBMCs) were cultured and exposed to the selected doses of A $\beta$ (25–35) peptide (10  $\mu$ M), GO (10  $\mu$ U/ml), and H<sub>2</sub>O<sub>2</sub> (50  $\mu$ M) for 24 h treatment period. A $\beta$ (25–35) peptide and GO exposure did not result in any cytotoxic effect on the PBMCs after 24 h treatment incubation as compared to the non-treated control cells (Fig. 1g); except a minimal cytotoxicity (~8%) was observed in H<sub>2</sub>O<sub>2</sub> treated PBMCs.

In addition, the non-cytotoxic nature of selected doses of oxidants was determined by PCNA protein expression analysis using Western blotting. C6 and U-87 MG cells treated with A $\beta$ (25–35) peptide (10  $\mu$ M), GO (10  $\mu$ U/ml), and H<sub>2</sub>O<sub>2</sub> (50  $\mu$ M) for 24 h and 48 h time periods showed an increase

in the level of PCNA protein when compared with non-treated control cells (Fig. 2).

### Non-cytotoxic concentrations of A $\beta$ (25–35), GO, and H<sub>2</sub>O<sub>2</sub> induces oxidative stress via enhancing cellular ROS level

Treatment of oxidants A $\beta$ (25–35) peptide, GO, and H<sub>2</sub>O<sub>2</sub> resulted in the generation of intracellular ROS which was measured using fluorescence dye-based H<sub>2</sub>DCFDA assay. Following exposure to A $\beta$ (25–35) peptide (10  $\mu$ M), GO (10  $\mu$ U/ml), and H<sub>2</sub>O<sub>2</sub> (50  $\mu$ M), a significant increase in ROS generation was observed at 24 h and 48 h time points in C6 and U-87 MG cells as compared to untreated control cells (Fig. 3).

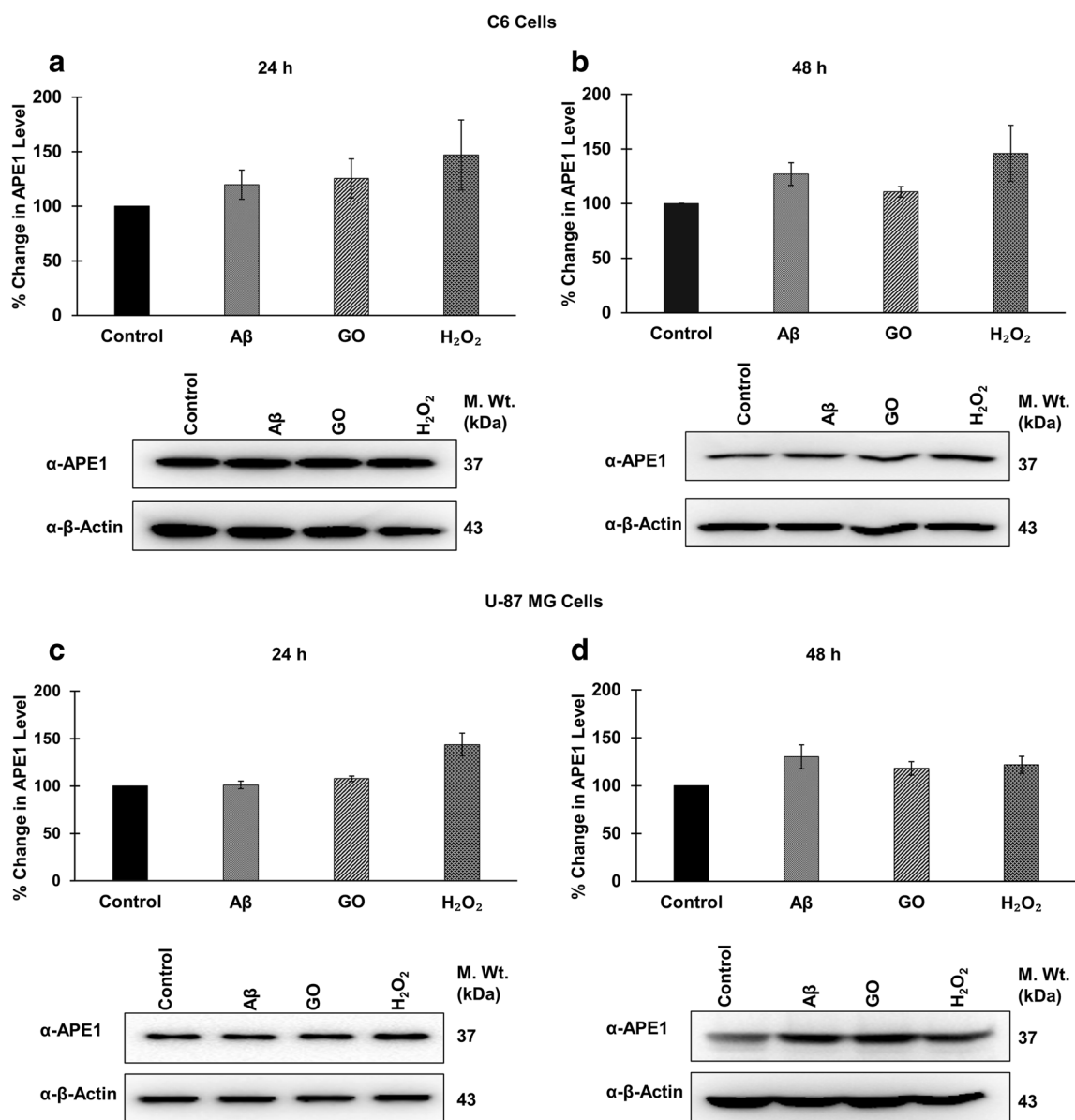


**Fig. 4** Western blot analysis of APE1 protein level in the total cell lysates of oxidatively stressed C6 cells (a & b) and U-87 MG cells (c & d). The results are expressed as a mean  $\pm$  standard deviation (n = 3)

## Oxidative stress elevates cellular and extracellular APE1 levels in C6 and U-87 MG cells

APE1 protein expression level in total cell lysates of C6 cells treated with A $\beta$ (25–35) peptide (10  $\mu$ M), GO (10  $\mu$ U/ml), and H<sub>2</sub>O<sub>2</sub> (50  $\mu$ M) for 24 h showed an increase by 20%, 25%, and 47%, respectively, when compared with untreated control C6 cells. Similarly, a further increase of 48 h exposure time of oxidants resulted in an increase in APE1 protein expression level by 27%, 11%, and 46%, respectively (Fig. 4a, b). 24 h treatment of GO and H<sub>2</sub>O<sub>2</sub> increased the protein expression level of APE1 by 8% and 44%, respectively, in U-87 MG cells, when compared with that of untreated control U-87 MG cells. U-87 MG cells treated with A $\beta$ (25–35) peptide for 24 h did not show any significant change in APE1 expression level. Further, increase in the exposure time of A $\beta$ (25–35) peptide, GO, and H<sub>2</sub>O<sub>2</sub> upto 48 h, increased the APE1 expression level by 30%, 18%, and 22%, respectively (Fig. 4c, d).

Further, the impact of oxidative stress on the extracellular secretion of APE1 in C6 and U-87 MG cells was evaluated using Western blotting. Extracellular secretion of APE1 was found to be time-dependent in C6 and U-87 MG cell culture conditioned media upon A $\beta$ (25–35) peptide, GO, and H<sub>2</sub>O<sub>2</sub> treatments (Fig. 5). A phenomenon recently discovered in

cancer research associated with APE1 with unexplored function(s).

## Oxidative stress enhances endonuclease (DNA repair) activity of APE1 in C6 and U-87 MG cells

APE1's DNA repair endonuclease activity was found to be increased by 19% (1.19 fold), 30% (1.3 fold), and 2.3 fold after 24 h treatment of A $\beta$ (25–35) peptide (10  $\mu$ M), GO (10  $\mu$ U/ml), and H<sub>2</sub>O<sub>2</sub> (50  $\mu$ M), respectively, in the nuclear extracts of C6 cells as compared to the non-treated control cells. Similarly, APE1's endonuclease activity was found to be increased by 33% (1.33 fold), 77% (1.77 fold), and 2 fold after 24 h treatment of A $\beta$ (25–35) peptide (10  $\mu$ M), GO (10  $\mu$ U/ml), and H<sub>2</sub>O<sub>2</sub> (50  $\mu$ M), respectively, in the nuclear extract of U-87 MG cells as compared to the non-treated control U-87 MG cells (Fig. 6).

## Oxidative stress modulates expression levels of BER-pathway enzymes

To understand the effect of oxidative stress on BER-pathway, the key enzymes associated with BER-pathway were analyzed at the protein level (Fig. 7a, f). As compared to untreated control cells, C6 cells treated with A $\beta$ (25–35) peptide

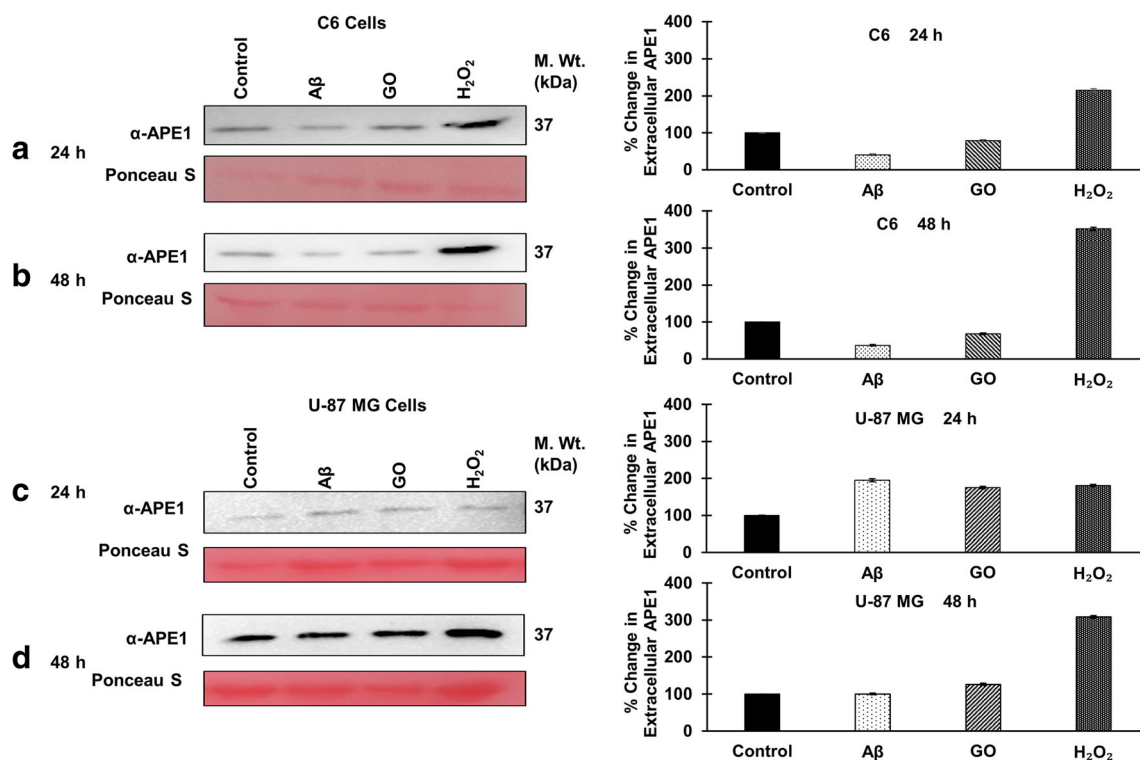


**Fig. 5** Oxidative stress induced extracellular secretion of APE1 upon stimulation with the oxidants A $\beta$ (25–35) peptide (10  $\mu$ M), GO (10  $\mu$ U/ml), and H<sub>2</sub>O<sub>2</sub> (50  $\mu$ M) in C6 (a & b) and U-87 MG (c & d) cells for 24 h and 48 h time points. Extracellular media was collected and filtered

through 0.2  $\mu$ m syringe filter and volume based i.e. 40  $\mu$ L of the clarified media was loaded in to each well along with the SDS-loading dye. Ponceau S was used as loading control for the normalization. The results are expressed as a mean  $\pm$  standard error ( $n = 2$ )

(10  $\mu$ M), GO (10  $\mu$ U/ml), and  $H_2O_2$  (50  $\mu$ M) for 24 h showed increase in the protein expression level of PARP1 by 1.5 fold, 2.5 fold, and 2.0 fold, respectively (Fig. 7b), and XRCC1 level was elevated by 1.75, 1.84, and 3.75 folds, respectively (Fig. 7c). Further, no change was observed in the expression level of DNA pol  $\beta$  in C6 cells for 24 h, however 48 h exposure increased the DNA pol  $\beta$  level by 2.0 fold, 3.85 fold, and 3.7 fold, respectively (Fig. 7d). C6 cells treated with  $H_2O_2$  for 24 h increased the ligase III $\alpha$  protein expression level by 18%, however, it was found to be decreased by 10% with GO treatment, and no change was observed upon A $\beta$ (25–35) peptide treatment (Fig. 7e).

U-87 MG cells treated with A $\beta$ (25–35) peptide (10  $\mu$ M), GO (10  $\mu$ U/ml), and  $H_2O_2$  (50  $\mu$ M) for 24 h increased PARP1 expression by 16%, 64%, and 6%, respectively (Fig. 7g) and XRCC1 expression level found to be increased in A $\beta$ (25–35) peptide treatment by 43%. A decrease in XRCC1 expression level was observed by 18%, and 12%, following treatment with GO, and  $H_2O_2$  for 24 h time point when compared to untreated control U-87 MG cells (Fig. 7h). Further, 24 h treatment of A $\beta$ (25–35) peptide increased the expression of DNA

pol  $\beta$  by 18%; however, no significant change was observed in the expression of DNA pol  $\beta$  in GO and  $H_2O_2$  treated U-87 MG cells (Fig. 7i). U-87 MG cells treated with 10  $\mu$ M A $\beta$ (25–35) for 24 h resulted in a slight increase in ligase III $\alpha$  expression level by 7%, and a significant decrease in its expression level was observed following treatment with GO and  $H_2O_2$  for 24 h time point (Fig. 7j).

### Oxidative stress modulates intracellular PKM2 levels

In order to understand about the non-glycolytic function of PKM2, Western blot analysis was performed to determine the expression level of PKM2 protein in C6 cells treated with A $\beta$ (25–35) peptide (10  $\mu$ M), and GO (10  $\mu$ U/ml) for 24 h, showed an increase by 35% (1.35 fold) and 8% (1.08 fold) respectively, when compared with untreated control C6 cells. However,  $H_2O_2$  (50  $\mu$ M) treatment for 24 h decreased the PKM2 protein level by 18% (1.18 fold) in C6 cells (Fig. 8a). C6 cells further exposed to A $\beta$ (25–35) peptide (10  $\mu$ M) for 48 h showed an increase in PKM2 protein level by 17% (1.17 fold) when compared to untreated control C6 cells. Whereas,

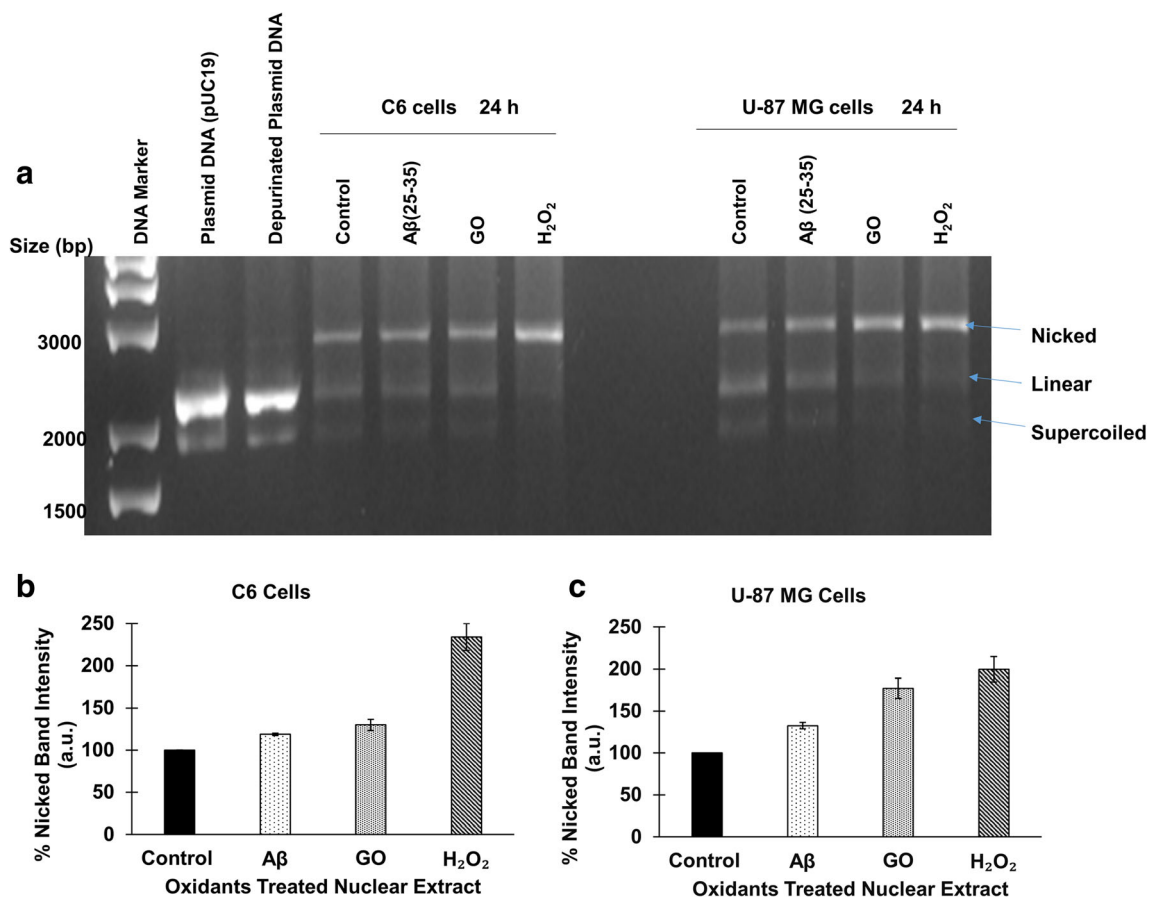


**Fig. 6** a Analysis of agarose gel based APE1's endonuclease (DNA repair) activity in nuclear extracts of C6 and U-87 MG cells treated with oxidants [10  $\mu$ M A $\beta$ (25–35) peptide, 10  $\mu$ U/ml GO, and 50  $\mu$ M  $H_2O_2$ ] after 24 h time point. Using depurinated pUC-19 plasmid DNA as a substrate, the AP

endonuclease activity was determined, and (b & c) the densitometry analysis of band intensities in C6 and U-87 MG cell nuclear extracts are presented as corresponding % nicked band intensity (a.u.). The results are expressed as mean  $\pm$  standard error (n = 2)

GO (10  $\mu$ U/ml) and H<sub>2</sub>O<sub>2</sub> (50  $\mu$ M) treatment to the C6 cells for 48 h time period did not show any change in PKM2 protein level (Fig. 8b). The level of PKM2 protein in U-87 MG cells treated with A $\beta$ (25–35) peptide (10  $\mu$ M), GO (10  $\mu$ U/ml) and H<sub>2</sub>O<sub>2</sub> (50  $\mu$ M) for 24 h showed an increase in the protein level of PKM2 by 33% (1.33 fold), 62% (1.62 fold) and 44% (1.44 fold), respectively. Similarly, further exposure of oxidants to U-87 MG for 48 h time point increased the PKM2 protein level by 27% (1.27 fold), 80% (1.8 fold), and 44% (1.44 fold),

respectively, as compared to untreated control U-87 MG cells (Fig. 8c, d).

### Oxidative stress stimulates ENPP2's intracellular expression and extracellular secretion

ENPP2's intracellular expression was monitored by Western blot analysis upon oxidative stress. In this study, the A $\beta$ (25–35) peptide treatment to U-87 MG cells for

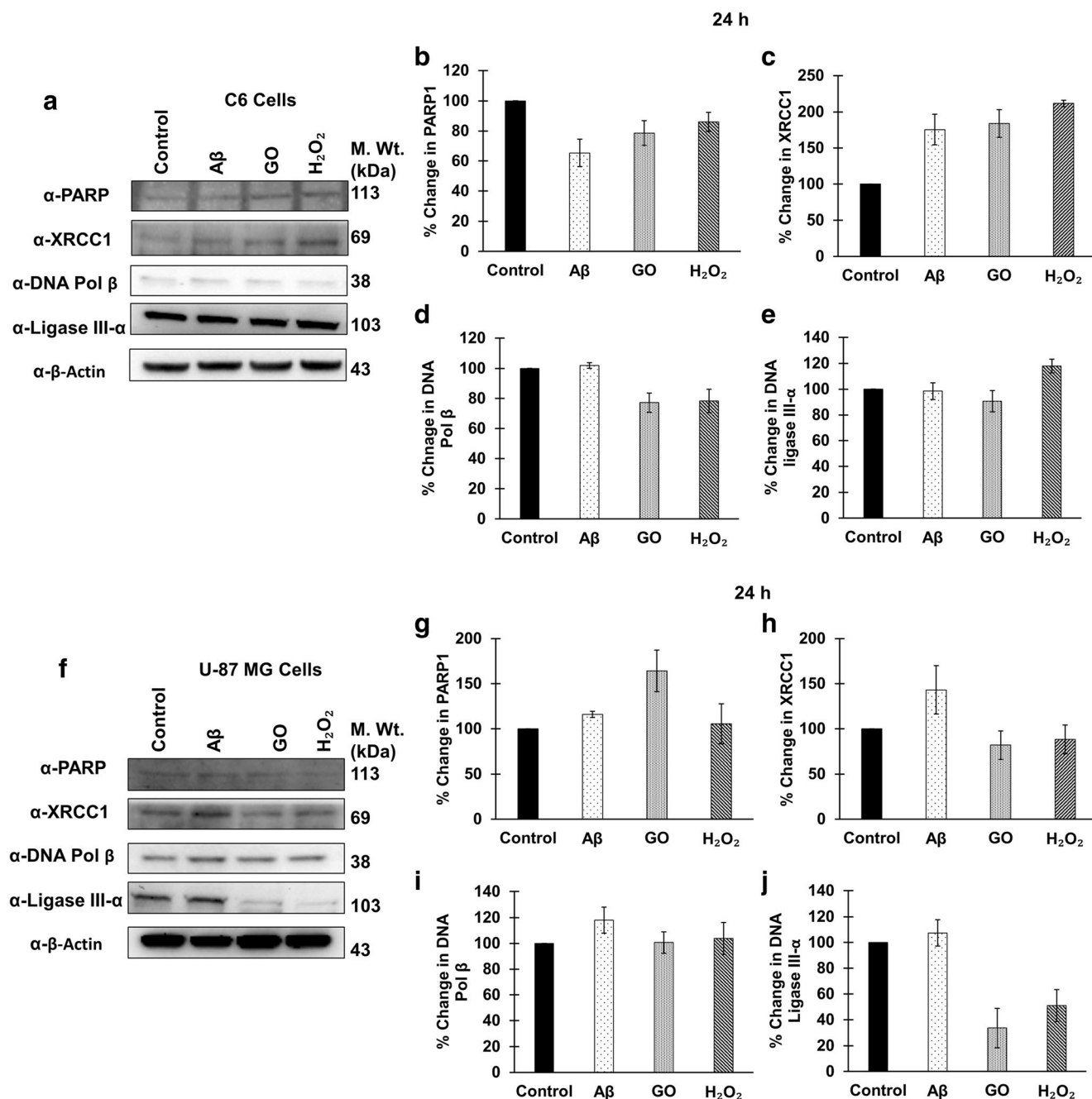


**Fig. 7** Western blot analysis using total cell lysates for oxidative stress induced changes in the expression level of BER-pathway enzymes upon stimulation with the oxidants A $\beta$ (25–35) peptide (10  $\mu$ M), GO (10  $\mu$ U/ml),

and H<sub>2</sub>O<sub>2</sub> (50  $\mu$ M) in C6 cells (a, b, c, d, & e) and U-87 MG cells (f, g, h, i, & j) for 24 h time period. The results are expressed as a mean  $\pm$  standard error (n = 2)

24 h time point did not show any significant change in ENPP2 level in total cell lysates. However, GO, and H<sub>2</sub>O<sub>2</sub> treatment resulted an increase by 43% (1.43 fold) and 58% (1.58 fold), respectively, as compared with non-treated control U-87 MG cell lysates (Fig. 9a). Further, 48 h exposure of A $\beta$ (25–35) peptide (10  $\mu$ M), GO (10  $\mu$ U/ml), and H<sub>2</sub>O<sub>2</sub> (50  $\mu$ M) resulted in 1.2 fold, 4.1 fold, and 11.5 fold increase in ENPP2 protein level, respectively (Fig. 9b).

Analysis of extracellular conditioned media by Western blotting showed extracellular ENPP2's secretion into the medium.

C6 cells treated with A $\beta$ (25–35) peptide (10  $\mu$ M), GO (10  $\mu$ U/ml), and H<sub>2</sub>O<sub>2</sub> (50  $\mu$ M) for 24 h time period resulted in an increase in the level of ENPP2 secretion into extracellular media, as compared with that of non-treated control C6 cell culture media. Similar trend of increase in secreted ENPP2 level in the extracellular media was observed in C6 cells after the treatment of A $\beta$ (25–35) peptide (10  $\mu$ M), GO (10  $\mu$ U/ml), and H<sub>2</sub>O<sub>2</sub> (50  $\mu$ M) for 48 h time period (Fig. 9c). U-87 MG cells incubated in the presence of A $\beta$ (25–35) peptide (10  $\mu$ M), GO (10  $\mu$ U/ml), and H<sub>2</sub>O<sub>2</sub> (50  $\mu$ M) for 24 h time period also

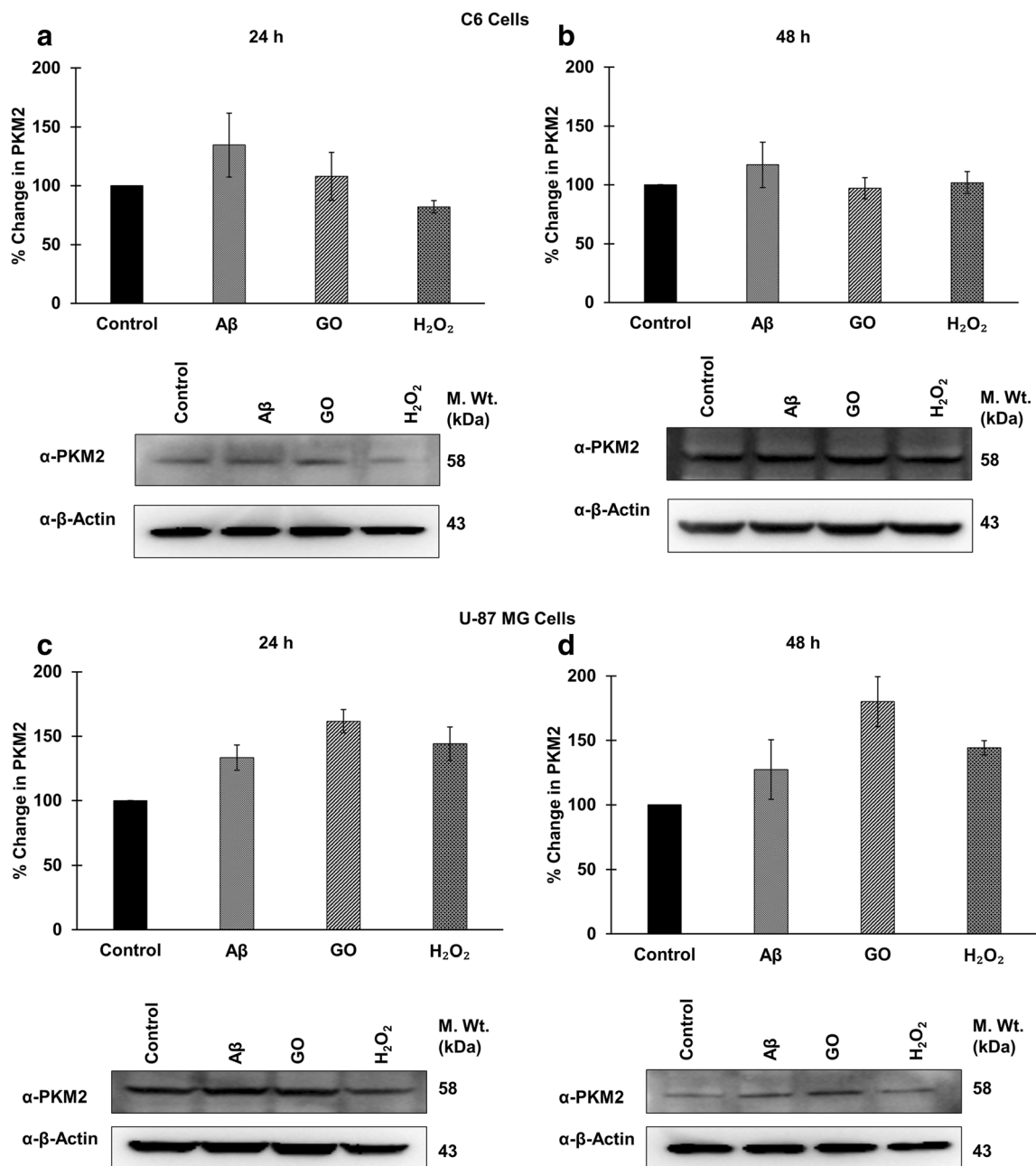


**Fig. 8** Western blot analysis of PKM2 protein level in the total cell lysates of C6 cells (a & b) and U-87 MG cells (c & d) treated with the oxidants [10  $\mu$ M A $\beta$ (25–35) peptide, 10  $\mu$ U/ml GO, and 50  $\mu$ M H<sub>2</sub>O<sub>2</sub>] for 24 h

and 48 h time points, respectively. The results are expressed as a mean  $\pm$  standard deviation (n = 3)

showed a significant increase in the secreted ENPP2 level in the extracellular culture media when compared with that of non-treated control U-87 MG cells culture media. Furthermore, U-87 MG cells treated with A $\beta$ (25–35) peptide (10  $\mu$ M), GO (10  $\mu$ U/ml), and H<sub>2</sub>O<sub>2</sub> (50  $\mu$ M) for 48 h time period increased the level of secreted ENPP2 in the extracellular media (Fig. 9d).

### Oxidative stress stimulates LysoPLD activity of ENPP2

ENPP2 produces bioactive lipid LPA extracellularly which acts as a signalling molecule in various cellular processes via its LysoPLD activity. Extracellular conditioned media of oxidative stress induced C6 and U-87 MG cells were used to analyze the LysoPLD activity of ENPP2. Time-dependent increase in the ENPP2's LysoPLD activity was observed. For 24 h oxidants treatment, an increase in LysoPLD activity of

ENPP2 in C6 cells was observed. Further increase in exposure time to 48 h resulted in significant increase in LysoPLD activity of ENPP2 (Fig. 9e). There was no change in the ENPP2's LysoPLD activity at 24 h time period of oxidants treated U-87 MG cells, and upon further increase in the exposure time of oxidants to 48 h, resulted in significant increase in the LysoPLD activity in U-87 MG cells as compared with that of untreated control U-87 MG cells (Fig. 9f).

### Oxidative stress modulates subcellular distribution and localization of APE1, PKM2, and ENPP2, and stimulates their cross-talk in C6 and U-87 MG cells

Upon establishing the role of oxidative stress in modulating the protein level (total cell lysates) of the three enzymes (APE1, PKM2, and ENPP2); and the endonuclease DNA repair function

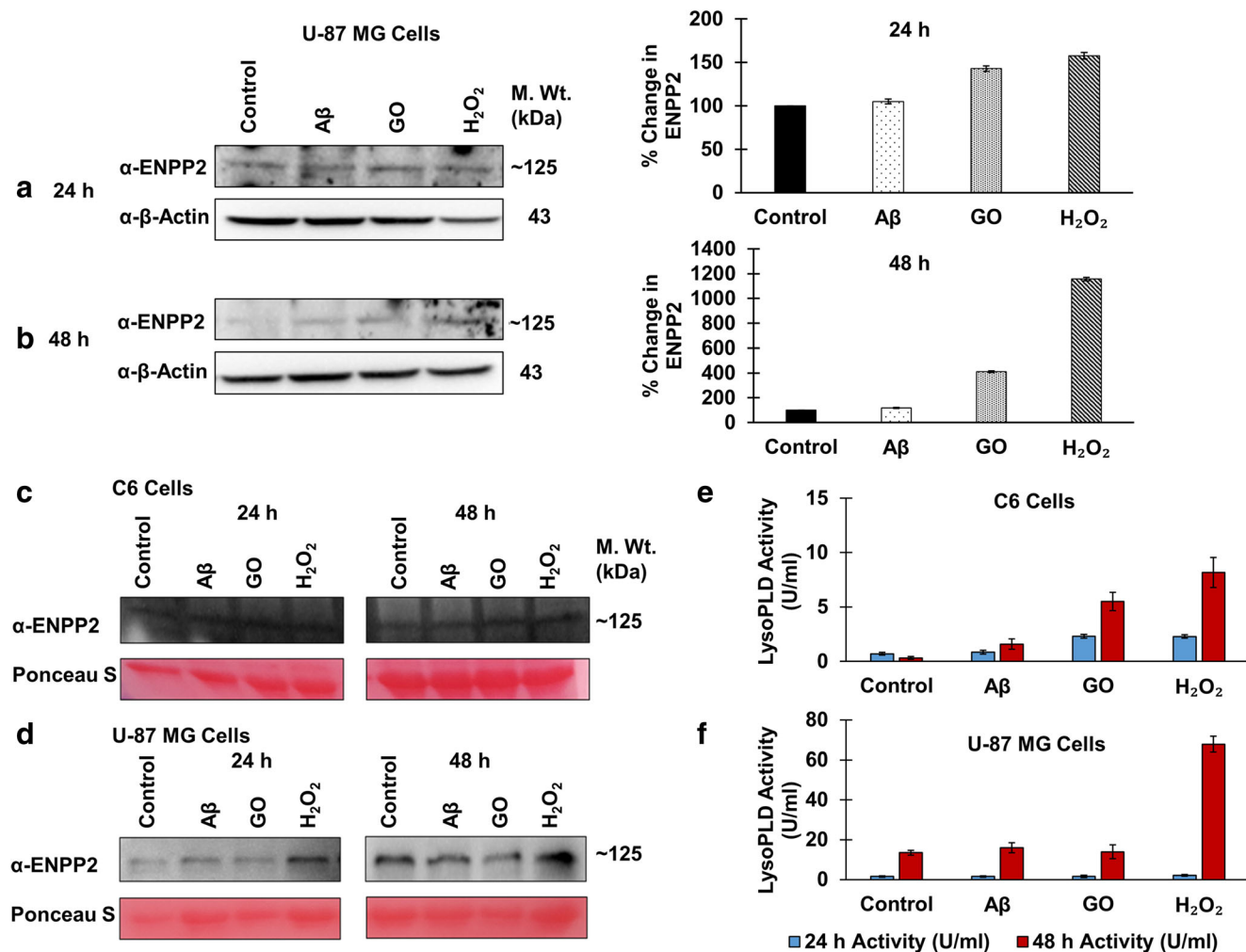


**Fig. 9** (a & b) Western blot analysis of ENPP2 protein level in the total cell lysates of the human glial U-87 MG cells treated with oxidants (10  $\mu$ M A $\beta$ (25–35), 10  $\mu$ U/ml GO, and 50  $\mu$ M H<sub>2</sub>O<sub>2</sub>) for 24 h and 48 h time points.  $\beta$ -Actin was used as loading control; (c & d) Western blot analysis of extracellular ENPP2's expression in the secretory media of the untreated control and in the oxidants: 10  $\mu$ M A $\beta$ (25–35), 10  $\mu$ U/ml GO and 50  $\mu$ M

H<sub>2</sub>O<sub>2</sub> for 24 h, and 48 h in C6 and U-87 MG cells, respectively. Ponceau S images were used for loading control and normalization [a–d: mean  $\pm$  standard error (n = 2)]; (e & f) ENPP2 activity assay in the secretory media of 10  $\mu$ M A $\beta$ (25–35), 10  $\mu$ U/ml GO and 50  $\mu$ M H<sub>2</sub>O<sub>2</sub> treated cells at 24 h and 48 h in secretory media of C6 cells and U-87 MG cells, respectively (n = 3)

of APE1 and LysoPLD activity of ENPP2, we further thought to determine any functional association between them towards aggressiveness of brain cancer. C6 and U-87 MG cells exposed to oxidants A $\beta$ (25–35) peptide (10  $\mu$ M), GO (10  $\mu$ U/ml), and H<sub>2</sub>O<sub>2</sub> (50  $\mu$ M) for 24 h and 48 h time points, resulted in an increased expression level of APE1, PKM2 and ENPP2 in both cytosolic and nuclear compartments as analyzed by immunofluorescence microscopy in C6 cells. Oxidants treatment for 24 h resulted in nuclear translocation of APE1, nuclear and cytoplasmic translocation of PKM2 and ENPP2. APE1 and PKM2 proteins were colocalized upon oxidants treatment for 24 h in C6 and U-87 MG cells as shown in merged images.

APE1 and PKM2 were found to be colocalized strongly upon treatment of GO. However, decreased colocalization of APE1 and PKM2 was observed in C6 and U-87 MG cells with the progress in treatment time point of oxidants to 48 h (Fig. 10a, b) advocating for early time point association for the non-glycolytic PKM2 function associated in the nucleus.

Further, the colocalization of APE1 with ENPP2 was also observed. Oxidants treatment for 24 h C6 cells and U-87 MG cells induced colocalization of APE1 with ENPP2. After 48 h of oxidants treatment in C6 and U-87 MG cells, a decrease in colocalization between APE1 with ENPP2 was observed (Fig. 11a, b).

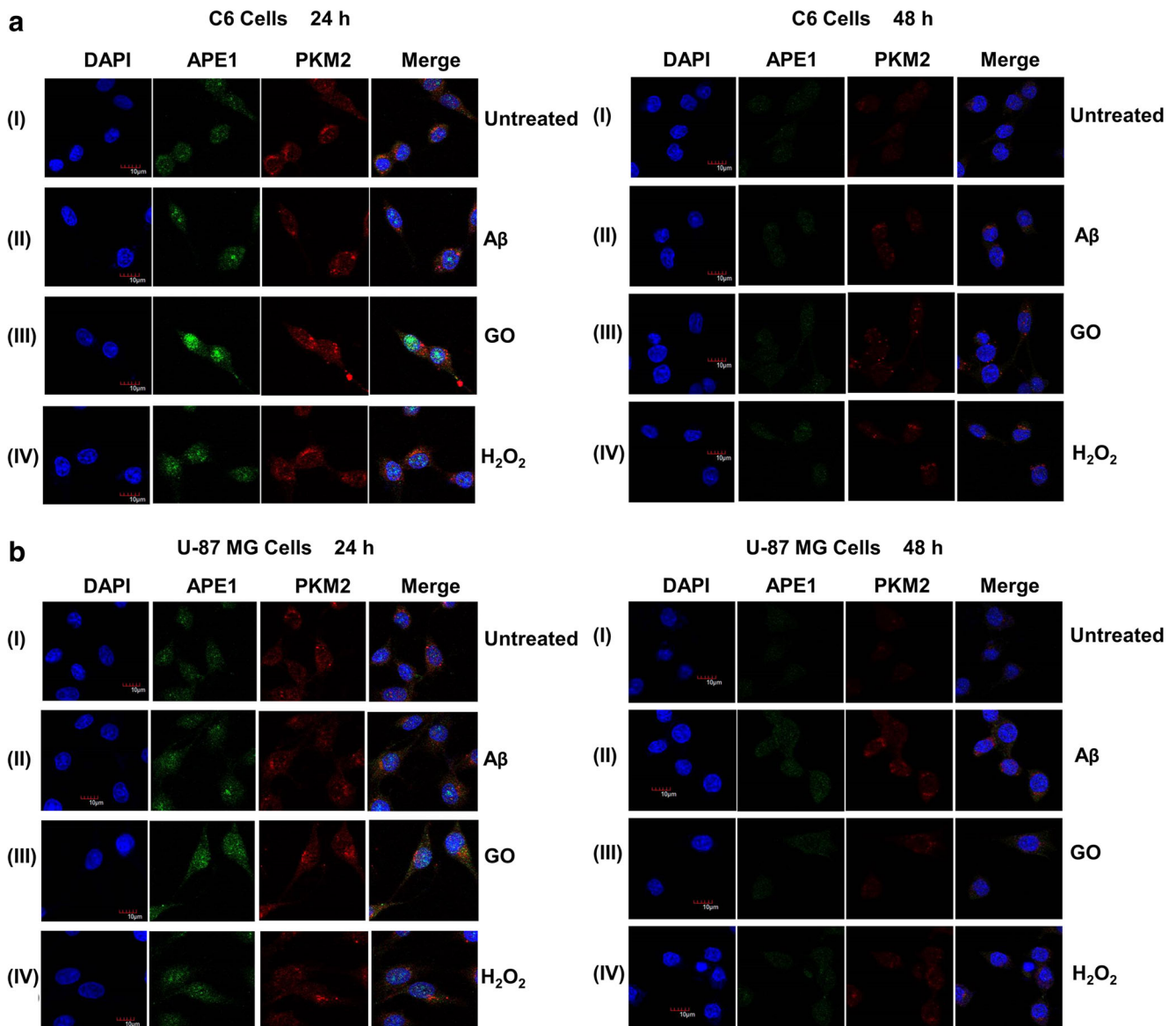


**Fig. 10** Association/Co-localization between APE1 and PKM2: Fluorescence immunocytochemistry of C6 (a) and U-87 MG cells (b) using antibodies against APE1 and PKM2; and probed with secondary antibodies labeled with fluorescent dye Alexa488 (Green) and Alexa647 (Red). Nuclear counter staining was performed using DAPI (Blue).

Representative micrographs of confocal laser scanning (60X) with Olympus microscope are presented from 24 h and 48 h time points for the untreated cells; 10  $\mu$ M A $\beta$ (25–35) peptide treated; 10  $\mu$ U/ml GO treated; and 50  $\mu$ M H<sub>2</sub>O<sub>2</sub> treated C6 and U-87 MG cells

Further, C6 and U-87 MG cells were analyzed for the crosstalk of these three proteins viz. APE1, PKM2 and ENPP2 upon 24 h and 48 h exposure of oxidants A $\beta$ (25–35) peptide, GO, and H<sub>2</sub>O<sub>2</sub>. The immunofluorescence images indicate an independent protein's expression (APE1, PKM2 and ENPP2) upon oxidative stress in C6 and U-87 MG cells. Further colocalization of APE1, PKM2 and ENPP2 was observed strongly at 24 h and were found to be stable upto 48 h time period in oxidants-treated C6 and U-87 MG cells, as compared with that of non-treated control cells as shown in merged images (Fig. 12a, b).

### LPA upregulates subcellular distribution and cross-talk (co-localization) between APE1 and ENPP2 in C6 and U-87 MG cells

Effect of LPA (10  $\mu$ M) was determined on APE1 and ENPP2 expression level in C6 and U-87 MG cells for 24 h and 48 h time points. Our results showed that C6 cells displayed a time-dependent increase in the cytoplasmic and nuclear expression of APE1 and ENPP2 upon LPA treatment for 24 h, and 48 h as compared to untreated control C6 cells. APE1 and ENPP2 were found to be colocalized strongly upon treatment of LPA at 48 h time point as analyzed using immunofluorescence

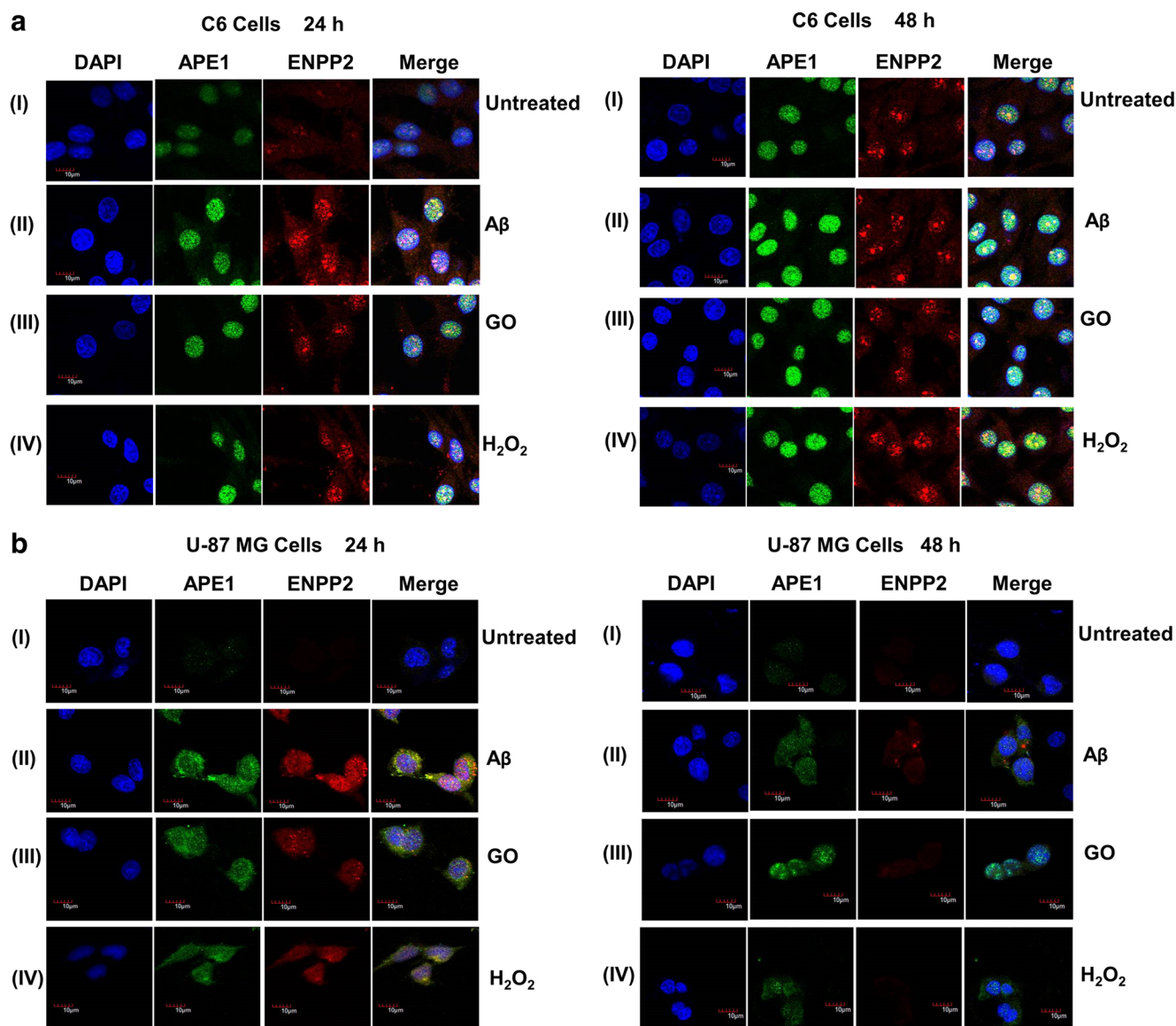


**Fig. 11** Association/Co-localization between APE1 and ENPP2: Fluorescence immunocytochemistry of C6 (a) and U-87 MG cells (b) using antibodies against APE1, and ENPP2; and probed with secondary antibodies labeled with fluorescent dye Alexa488 (Green) and Alexa647 (Red). Nuclear counter staining was performed using DAPI (Blue).

Representative micrographs of confocal laser scanning (60X) with Olympus microscope are represented from the oxidants A $\beta$ (25–35), GO, and H<sub>2</sub>O<sub>2</sub> treatments for 24 h and 48 h time point for control and oxidants treated C6 and U-87 MG cells

microscopy (Fig. 13a). A similar finding was observed in the U-87 MG cells upon LPA for 24 h, and 48 h time points (Fig. 13b). These results suggested that LPA causes feedback upregulation of ENPP2 expression and cross-talk between APE1 and ENPP2 proteins in C6 and U-87 MG cells.

### LPA also stimulates cellular migration in C6 and U-87 MG cells

LPA (10  $\mu$ M) treatment for 24 h induced cellular migration in the C6 cells as analyzed by the Wound healing assay, which shows complete closure of the cell-free gap as compared to the untreated control cells. An increase in cell migration was noted in GO and H<sub>2</sub>O<sub>2</sub> treated C6 cells by 12% and 31%, respectively; and the A $\beta$ (25–35) peptide treatment inhibited the cellular migration marginally as compared to untreated control

C6 cells. However, LPA treatment along with the A $\beta$ (25–35) peptide-induced cellular migration by 64% (1.64 fold), when compared with that of untreated control C6 cells. LPA treatment along with the treatment of GO induced cellular migration by 2.25 folds as compared to the untreated control C6 cells. 24 h LPA treatment along with H<sub>2</sub>O<sub>2</sub> treatment also increased the cellular migration by 63% (1.63 fold) when compared to untreated control C6 cells (Fig. 14a).

U-87 MG cells were treated with LPA for 24 h and analyzed by the wound healing assay which showed complete closure of the cell-free gap as compared with that of untreated control U-87 MG cells. A $\beta$ (25–35) peptide treatment to the U-87 MG cells showed negligible change in cellular migration as compared with that of non-treated control U-87 MG cells. However, an increase in cell migration was observed in GO treated cells by 46%; and

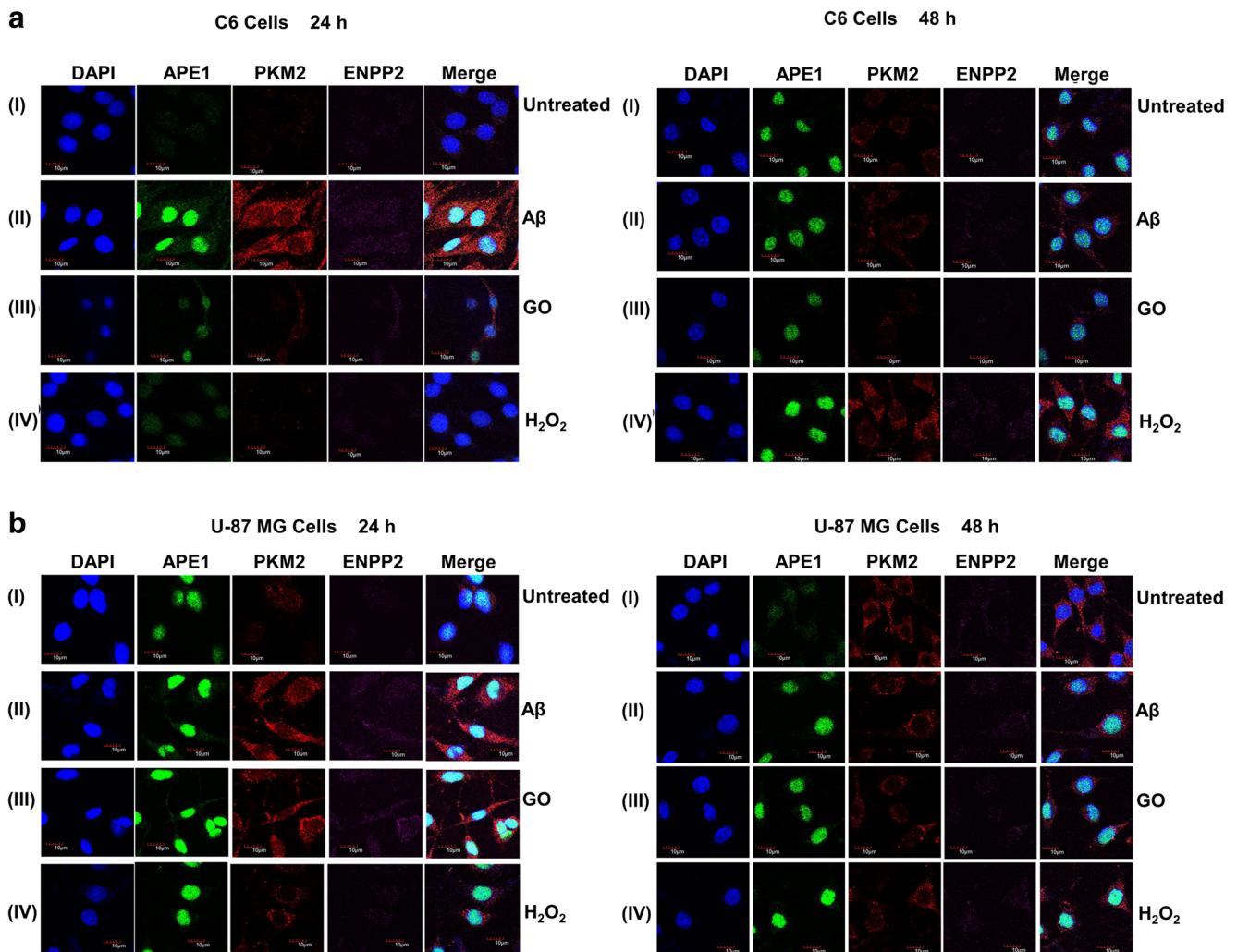


**Fig. 12** Association/Co-localization/Cross-talk between APE1, PKM2, and ENPP2: Fluorescence immunocytochemistry of C6 (a) and U-87 MG cells (b) using antibodies against APE1, PKM2, and ENPP2; and probed with secondary antibodies labeled with fluorescent dye Alexa488 (Green), Alexa568 (Magenta) and Alexa647 (Red). Nuclear counter

staining was performed using DAPI (Blue). Representative micrographs of confocal laser scanning (60X) with Olympus microscope are presented from the A $\beta$ (25–35), GO, and H<sub>2</sub>O<sub>2</sub> treatments for 24 h and 48 h time points for control and oxidants treated C6 and U-87 MG cells

H<sub>2</sub>O<sub>2</sub> treated cells showed inhibition in the migration of U-87 MG cells as compared to the untreated control cells. Surprisingly, alone LPA treatment showed 4 folds increase in U-87 MG cell migration as compared with that of untreated control U-87 MG cells. LPA treatment in combination with A $\beta$ (25–35) peptide resulted in 2.7 folds increase in cell migration with respect to the non-treated control U-87 MG cells. LPA in combination with A $\beta$ (25–35) peptide increased U-87 MG cell migration to 2.5 folds when compared only with that of A $\beta$ (25–35) peptide treated U-87 MG cells. LPA in combination with GO, induced 2.7 folds to increase in U-87 MG cell migration as compared with that of untreated control U-87 MG cells. Further, LPA treatment in combination with H<sub>2</sub>O<sub>2</sub> induced cell migration by 2.6 folds when compared to untreated U-87 MG cells, and 3.7 folds increase in cell migration was observed following LPA treatment in combination with H<sub>2</sub>O<sub>2</sub> when compared with that of only H<sub>2</sub>O<sub>2</sub>-treated U-87 MG cells at 24 h time point (Fig. 14b). The present results advocates for the role of oxidative stress in association with the bioactive LPA towards the migratory behavior of C6 and U-87 MG cells.

## Discussion

GBM is a high-grade astrocytoma which is the most common and lethal primary tumors of the CNS. Patients suffering from GBM have a median survival of less than 1 year after treatment with multi-model therapies (Babu et al. 2016; Capdevila et al. 2017). In order to explore the injurious mechanism(s) underlying GBM, the current study focused on the role of elevated oxidative stress in rat glioma C6 cells and human glioblastoma U-87 MG cells, induced by three model oxidants viz. A $\beta$ (25–35) peptide, GO, and H<sub>2</sub>O<sub>2</sub> (non-cytotoxic concentrations), in

the regulation of cellular key proteins viz. APE1, PKM2, and ENPP2. Oxidative stress leads to the redox imbalance in cancer cells as compared to the normal cells, which correlates with oncogenic stimulation in cancer cells (Valko et al. 2006). Due to accelerated and altered metabolism in cancer cells, there is increased ROS production (Sosa et al. 2013) which causes oxidative stress and oxidative damage to cellular structures manifesting into high proliferative rate of cancer cells (Choi et al. 2016). Non-cytotoxicity of the oxidants was further confirmed using Western blotting via analyzing the PCNA level for different time points (24 h and 48 h). PCNA is an important marker of cell proliferation and play an important role in the replication, repair machinery, and interacts with proteins involved in the cell cycle progression (Kelman 1997). In various research studies, PCNA level has also been correlated with the tumor progression and antiproliferative activities of cell cycle inhibitors (Costa et al. 2013; Dai and Zhang 2009; Sabarinathan et al. 2011).

Pyruvate kinase, which catalyzes the final step of glycolysis, has emerged as a potential regulator of the metabolic phenotype (Chaneton and Gottlieb 2012). It serves as the gatekeeper of cell growth and survival (Harris et al. 2012). Along with the metabolic function, PKM2 is also involved in the non-glycolytic functions. Translocation of the PKM2 to the nucleus leads to activation of various transcription factors endowing cancer cells with survival and growth advantages (Tamada et al. 2012). The PKM2 expression is necessary for aerobic glycolysis which is advantageous for the tumor cells (Cortés-Cros et al. 2013). In glioblastoma, isoform switching has been observed in PKM1 to PKM2 (Desai et al. 2014). In the present study, the PKM2 level was found to be increased upon the oxidative stress induced by the treatment of noncytotoxic doses of oxidants. Immunocytochemistry staining further confirmed PKM2 elevation in C6 and U-87 MG cells in the subcellular localization and

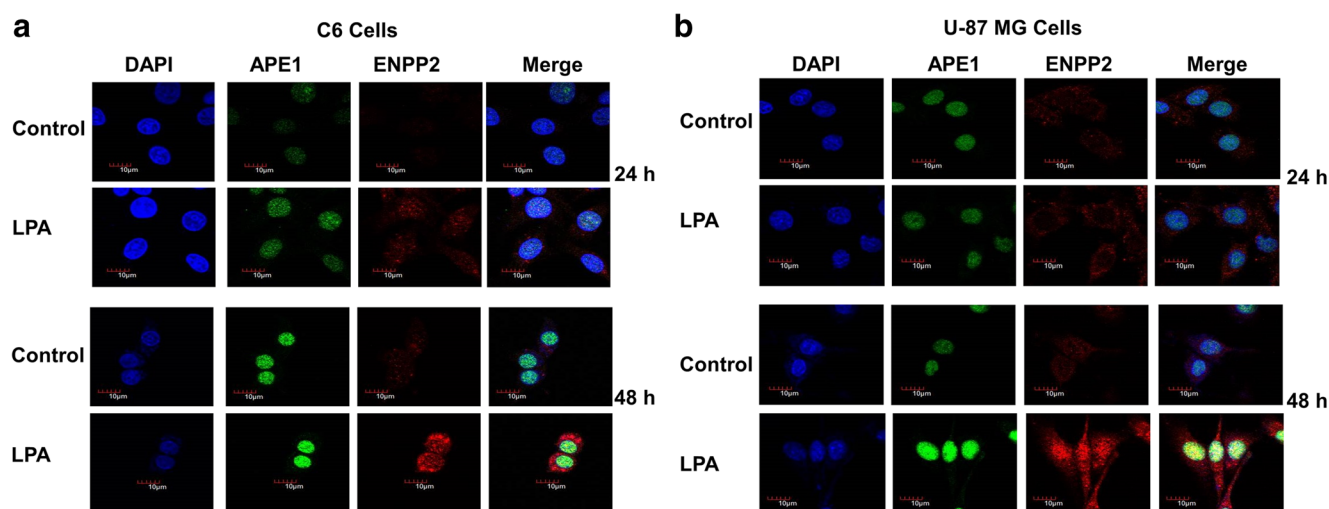


**Fig. 13** Association/Co-localization between APE1 and ENPP2: Fluorescence immunocytochemistry of C6 (a) and U-87 MG cells (b) using antibodies against APE1, and ENPP2; and probed with secondary antibodies labeled with fluorescent dye Alexa488 (Green) and Alexa647

(Red). Nuclear counter staining was performed using DAPI (Blue). Representative micrographs of confocal laser scanning (60X) with Olympus microscope are represented from 24 h and 48 h time point for control and 10  $\mu$ M LPA treated C6 and U-87 MG cells

also in the nucleus upon oxidative stress. In response to oxidative stress, PKM2 activity gets inhibited and enhances its binding with the SIRT5 resulting in stimulation in cell proliferation and growth (Xiangyun and Xiaomin 2017). Recently it has been suggested that increased oxidative stress is associated with mitochondrial translocation of PKM2 and its interaction with Bcl2 inhibiting apoptosis and enhancing glioblastoma cell survival (Liang et al. 2017). Various studies have also confirmed PKM2 activity as the deciding factor for the cancer cell survival or growth (Costa et al. 2013). In the present study, oxidative stress resulted in the colocalization of PKM2 and APE1 in response to oxidative stress in C6 and U-87 MG cells. Previously it has been reported that PKM2 forms stable (binary) interaction with APE1 in the neuronal cells against A $\beta$ (25–35) stress

(Mantha et al. 2012). Further increase in the oxidants exposure time resulted in decreased colocalization of APE1 and PKM2. Our data suggest for the colocalization of APE1 and PKM2 during the early period of the oxidative stress, which might have associated with the non-glycolytic function of PKM2 in the nuclear region. However, further studies in deciphering the same are required for better understanding of the interactions between APE1 and PKM2.

ENPP2 has been found to be highly expressed in the GBM SNB-78 cells (Kishi et al. 2006). The present study also explored the role of ENPP2 in the glioma cells subjected to the oxidative stress. The present study demonstrates that ENPP2's expression and secretion is stimulated by the oxidative stress and to be in a positive feedback mechanism for the ENPP2's

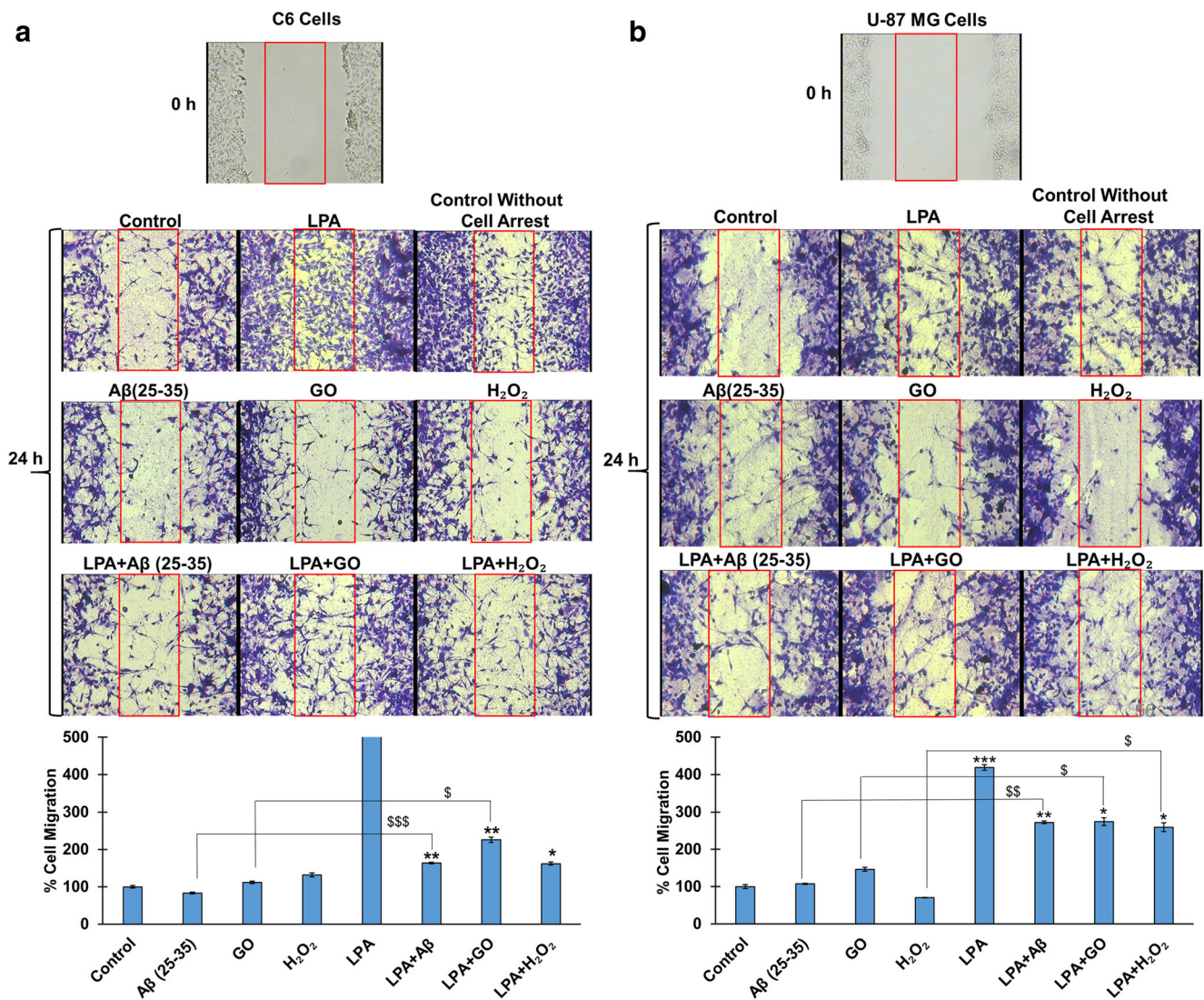


**Fig. 14** LPA induced cell migration in (a) C6 and (b) U-87 MG cells. Analysis of cell migration in LPA treatment and LPA in combination with the selected oxidants treatment in C6 and U-87 MG cells for 24 h time point. Cells were stained with methylene blue and images were captured using 10X objective lens of an inverted microscope (Olympus) equipped with video-camera from three random areas. The marked red area shows

cell migration in the central area of the cell-free space as compared to the 0 h control cells. The results are expressed as a mean  $\pm$  standard deviation (n = 3). Student's t-test was performed to evaluate the significance of the results. \*p  $\leq$  0.05, and \*\*p  $\leq$  0.01 represents comparison with untreated control cells; and \$p  $\leq$  0.05, and \$\$\$p  $\leq$  0.001 represents the significance level compared with oxidants treated cells

expression in C6 and U-87 MG cells. In microglial cells, it was reported earlier that  $H_2O_2$  (100  $\mu$ M) induces ENPP2 expression, and this overexpressed ENPP2 reduces the ROS level, carbonylated protein accumulation, proteasomal activity and catalase expression in mouse microglial BV2 and EOC cell lines and therefore, has been suggested for novel antioxidant role of endogenous ENPP2 expression at the brain level (Awada et al. 2012). In the present study, treatment of oxidants resulted in secretion of ENPP2 in the extracellular media in C6 and U-87 MG cells up to 48 h. The present study also reports that oxidative stress stimulates ENPP2 synthesis and secretion by C6 and U-87 MG. ROS generation also stimulated the ENPP2 expression and its LysoPLD activity in a time-dependent manner. Further, it is also attributed that ENPP2's bioactive product LPA mediates cell survival, proliferation, migration, wound healing and tissue remodeling. LPA acts as an inflammatory mediator in the tumor microenvironment that promotes cancer progression and promotes resistance to chemotherapy and radiotherapy (Benesch et al. 2014).

Various reports also advocates for the potential role of LPA towards the metastatic potential in various cancer cells (Kishi et al. 2006; Shida et al. 2003; Umezū-Goto et al. 2002; Yamada et al. 2004). It is reported that ENPP2 induces an invasive potential in the glioblastoma cells via LPA production. LPA is a growth factor-like lipid mediator that regulates many cellular functions. ENPP2 expressing cells invade through the oligodendrocyte monolayer significantly as compared to the ENPP2 depleted cells (Hoelzinger et al. 2008). In the present study, migratory behavior of C6 and U-87 MG cells was analyzed and it was found that LPA (10  $\mu$ M) displays a strong migratory potential in the C6 and U-87 MG cells and also stimulates cellular migration upon induction of oxidative stress in C6 and U-87 MG cells. Results of the present study was also supported by the findings displaying strong migratory response to LPA (10  $\mu$ M) and LPC (10  $\mu$ M) in SNB-78 cells (Kishi et al. 2006). Various reports also advocate for the role of LPA in stimulation of migration response in ovarian cancer SKOV-3 cells at 20  $\mu$ M (Hu et al. 2001) and the GBM SNB-78 cells via promoting the chemotactic response (Kishi et al. 2006). Our study demonstrated that the LPA treatment causes feedback regulation on ENPP2 expression in C6 and U-87 MG cells and acts as an activator for the ENPP2 protein expression. However, Benesch et al. 2015 showed that LPA suppresses the expression of ENPP2 and this inhibition is ineffective at the high concentration of LPC that occur in vivo. Also, the present study demonstrated that LPA treatment strongly induces colocalization of APE1 and ENPP2 in C6 and U-87 MG cells.

From the literature it is evident that elevated activity of APE1 is associated with GBM (Bobola et al. 2001) and oxidative stress has been accounted for its role in elevation of APE1 activity in GBM which also contribute towards the resistance of alkylating agents (Johannessen and Bjerkvig 2012; Silber et al. 2002). In the present study, induced oxidative stress in U-87

MG and C6 cells resulted in stimulation of BER-pathway enzyme APE1, which is involved in the repair of AP sites, and also a reductive activator of various transcription factors as reviewed extensively (Bhakat et al. 2009; Tell et al. 2009). In the present study, it is identified that upon oxidative stress, in addition to increased endogenous expression of APE1 (Cholia et al. 2017), its secretion into the extracellular media. The secretory APE1 levels in the extracellular medium of oxidatively-stressed C6 and U-87 MG cells were found to be increased time-dependently, which was also earlier documented (Choi et al. 2013) having unknown biological functions. Recently, it is also discovered that extracellular APE1 induces the production and secretion of the pro-inflammatory cytokine IL-6 in monocytic cells through the transactivation of NF- $\kappa$ B which may have a key role in APE1's inflammatory response in cancer progression (Nath et al. 2017). The importance of extracellular APE1 lies in the regulation of cellular functions such as apoptosis as it was reported that secreted acetylated APE1 triggers apoptosis in triple negative breast cancer BT-459 and MDA-MB-468 cells resistant to standard chemotherapeutic agents via binding to advanced glycation end products [RAGE] (Lee et al. 2015). The present study indicates that moderate level of oxidative stress results in an increased expression level, activity, and extracellular secretion of APE1, which clearly reveals that oxidative stress conditions might have effect on the APE1 functioning in C6 and U-87 MG cells that may be associated with the aggressiveness of GBM as suggested earlier (Montaldi et al. 2015). These results are also supported by the finding from the current and previous studies which also determined the ROS-dependent elevation in the APE1 level and its AP endonuclease activity (Silber et al. 2002; Cholia et al. 2017). Cross-talk or possible physical association of ENPP2 and APE1 in C6 and U-87 MG cells was analyzed using colocalization studies. In the present study, oxidative stress resulted in the colocalization of ENPP2 and APE1 in response to oxidative stress for different time points in C6 and U-87 MG cells. With further increase in exposure time increase in the colocalization of APE1, ENPP2 and the PKM2 was observed. Our data suggests for the cross-talk between the three enzymes viz. APE1, PKM2 and ENPP2. Oxidative stress responses might be the underlined route/mechanism(s) through which GBM and other cancer types might be advancing.

## Summary and conclusion

Aberrant ROS production in the tumor cells aggravate cancer incidence. The current study explored the role of oxidative stress using C6 and U-87 MG cell lines as a model system to evaluate the ROS-mediated regulation of three key enzymes associated with various cellular functions viz.: APE1, PKM2, and ENPP2. The results clearly suggest the progression of brain cancer via modulating the expression levels,

activity, and the association between these three enzymes. Based on these observation this study can also be extended to other high metastatic and aggressive cancers such as lung and breast cancers with additional focused studies.

**Acknowledgements** This work is supported to A.K.M. by the BSR-startup grant received from the University Grants Commission (UGC), New Delhi, India, and the funds received under the scheme Research Seed Money (RSM) from the Central University of Punjab, Bathinda (CUPB). R.P.C. acknowledges financial support in the form of a senior research fellowship (SRF) from the Indian Council for Medical Research (ICMR), New Delhi, India. The confocal laser scanning microscope (Olympus) facility of the Central Instrumentation Laboratory (CIL), CUPB is thankfully acknowledged. Because of the limited focus of the article, many relevant and appropriate references could not be included, for which the authors apologize.

## Compliance with ethical standards

**Conflict of interest** Authors declare that no conflict of interest exists.

## References

- Alía M, Ramos S, Mateos R, Granado-Serrano AB, Bravo L, Goya L (2006) Quercetin protects human hepatoma HepG2 against oxidative stress induced by tert-butyl hydroperoxide. *Toxicol Appl Pharmacol* 212:110–118
- Awada R, Rondeau P, Grès S, Saulnier-Blache JS, d'Hellencourt CL, Bourdon E (2012) Autotaxin protects microglial cells against oxidative stress. *Free Radic Biol Med* 52:516–526
- Babu R, Komisarow JM, Agarwal VJ, Rahimpour S, Iyer A, Britt D, Karikari IO, Grossi PM, Thomas S, Friedman AH (2016) Glioblastoma in the elderly: the effect of aggressive and modern therapies on survival. *J Neurosurg* 124:998–1007
- Benesch MG, Ko YM, McMullen TP, Brindley DN (2014) Autotaxin in the crosshairs: taking aim at cancer and other inflammatory conditions. *FEBS Lett* 588:2712–2727
- Benesch MG, Zhao YY, Curtis JM, McMullen TP, Brindley DN (2015) Regulation of autotaxin expression and secretion by lysophosphatidate and sphingosine 1-phosphate. *J Lipid Res* 56:1134–1144
- Bhakat K, Mantha A, Mitra S (2009) Transcriptional regulatory functions of mammalian AP-endonuclease (APE1/ref-1), an essential multi-functional protein. *Antioxid Redox Signal* 11:621–637
- Bobola MS, Blank A, Berger MS, Stevens BA, Silber JR (2001) Apurinic/apyrimidinic endonuclease activity is elevated in human adult gliomas. *Clin Cancer Res* 7:3510–3518
- Capdevila C, Rodriguez Vazquez L, Marti J (2017) Glioblastoma Multiforme and adult neurogenesis in the ventricular-subventricular zone: a review. *J Cell Physiol* 232:1596–1601
- Chaneton B, Gottlieb E (2012) Rocking cell metabolism: revised functions of the key glycolytic regulator PKM2 in cancer. *Trends Biochem Sci* 37:309–316
- Chen DS, Herman T, Demple B (1991) Two distinct human DNA diesterases that hydrolyze 3'-blocking deoxyribose fragments from oxidized DNA. *Nucleic Acids Res* 19:5907–5914
- Choi S, Lee YR, Park MS, Joo HK, Cho EJ, Kim HS, Kim CS, Park JB, Irani K, Jeon BH (2013) Histone deacetylases inhibitor trichostatin a modulates the extracellular release of APE1/ref-1. *Biochem Biophys Res Commun* 435:403–407
- Choi E-O, Jeong J-W, Park C, Hong SH, Kim G-Y, Hwang H-J, Cho E-J, Choi YH (2016) Baicalein protects C6 glial cells against hydrogen peroxide-induced oxidative stress and apoptosis through regulation of the Nrf2 signaling pathway. *Int J Mol Med* 37:798–806
- Cholia RP, Kumari S, Kumar S, Kaur M, Kaur M, Kumar R, Dhiman M, Mantha AK (2017) An in vitro study ascertaining the role of H<sub>2</sub>O<sub>2</sub> and glucose oxidase in modulation of antioxidant potential and cancer cell survival mechanisms in glioblastoma U-87 MG cells. *Metab Brain Dis* 32:1705–1716
- Cortés-Cros M, Hemmerlin C, Ferretti S, Zhang J, Gounarides JS, Yin H, Muller A, Haberkorn A, Chene P, Sellers WR (2013) M2 isoform of pyruvate kinase is dispensable for tumor maintenance and growth. *Proc Natl Acad Sci* 110:489–494
- Costa B, Bendinelli S, Gabelloni P, Da Pozzo E, Daniele S, Scatena F, Vanacore R, Campiglia P, Bertamino A, Gomez-Monterrey I (2013) Human glioblastoma multiforme: p53 reactivation by a novel MDM2 inhibitor. *PLoS One* 8:e72281
- Dai R, Zhang S (2009) Expressions and their significance of PTTG and PCNA proteins in glioma. *Chin-Ger J Clin Oncol* 8:110–113
- Desai S, Ding M, Wang B, Lu Z, Zhao Q, Shaw K, Yung WA, Weinstein JN, Tan M, Yao J (2014) Tissue-specific isoform switch and DNA hypomethylation of the pyruvate kinase PKM gene in human cancers. *Oncotarget* 5:8202
- Desmaret S, Qian L, Vanloo B, Meerschaert K, Van Damme J, Grooten J, Vandekerckhove J, Prestwich GD, Gettemans J (2005) Lysophosphatidic acid affinity chromatography reveals pyruvate kinase as a specific LPA-binding protein. *Biol Chem* 386:1137–1147
- Dhiman M, Zago MP, Nunez S, Amoroso A, Rementería H, Dousset P, Nunez Burgos F, Garg NJ (2012) Cardiac-oxidized antigens are targets of immune recognition by antibodies and potential molecular determinants in chagas disease pathogenesis. *PLoS One* 7(1):e28449
- Duthie S, Collins A, Duthie G, Dobson V (1997) Quercetin and myricetin protect against hydrogen peroxide-induced DNA damage (strand breaks and oxidised pyrimidines) in human lymphocytes. *Mutation Research/Genetic Toxicology and Environmental Mutagenesis* 393:223–231
- Fukushima N, Weiner JA, Chun J (2000) Lysophosphatidic acid (LPA) is a novel extracellular regulator of cortical neuroblast morphology. *Dev Biol* 228:6–18
- Harris I, McCracken S, Mak TW (2012) PKM2: a gatekeeper between growth and survival. *Cell Res* 22:447–449
- Hausmann J, Perrakis A, Moolenaar WH (2013) Structure-function relationships of autotaxin, a secreted lysophospholipase D. *Advances in Biological Regulation* 53:112–117
- Hoelzinger DB, Nakada M, Demuth T, Rosensteel T, Reavie LB, Berens ME (2008) Autotaxin: a secreted autocrine/paracrine factor that promotes glioma invasion. *J Neuro-Oncol* 86:297–309
- Hu Y-L, Tee M-K, Goetzl EJ, Auersperg N, Mills GB, Ferrara N, Jaffe RB (2001) Lysophosphatidic acid induction of vascular endothelial growth factor expression in human ovarian cancer cells. *J Natl Cancer Inst* 93:762–767
- Johannessen T-CA, Bjerkvig R (2012) Molecular mechanisms of temozolomide resistance in glioblastoma multiforme. *Expert Rev Anticancer Ther* 12:635–642
- Katsifa A, Kaffe E, Nikolaidou-Katsaridou N, Economides AN, Newbigging S, McKerlie C, Aidinis V (2015) The bulk of autotaxin activity is dispensable for adult mouse life. *PLoS One* 10:e0143083
- Kelman Z (1997) PCNA: structure, functions and interactions. *Oncogene* 14:629–640
- Kishi Y, Okudaira S, Tanaka M, Hama K, Shida D, Kitayama J, Yamori T, Aoki J, Fujimaki T, Arai H (2006) Autotaxin is overexpressed in glioblastoma multiforme and contributes to cell motility of glioblastoma by converting lysophosphatidylcholine to lysophosphatidic acid. *J Biol Chem* 281:17492–17500
- Lee YR, Kim KM, Jeon BH, Choi S (2015) Extracellularly secreted APE1/ref-1 triggers apoptosis in triple-negative breast cancer cells

- via RAGE binding, which is mediated through acetylation. *Oncotarget* 6:23383
- Liang J, Cao R, Wang X, Zhang Y, Wang P, Gao H, Li C, Yang F, Zeng R, Wei P (2017) Mitochondrial PKM2 regulates oxidative stress-induced apoptosis by stabilizing Bcl2. *Cell Res* 27:329–351
- Mantha AK, Dhiman M, Taglialatela G, Perez-Polo RJ, Mitra S (2012) Proteomic study of amyloid beta (25–35) peptide exposure to neuronal cells: impact on APE1/ref-1's protein–protein interaction. *J Neurosci Res* 90:1230–1239
- Mazurek S (2011) Pyruvate kinase type M2: a key regulator of the metabolic budget system in tumor cells. *Int J Biochem Cell Biol* 43:969–980
- Mazurek, S., Boschek, C. B., Hugo, F., & Eigenbrodt, E. (2005). Pyruvate kinase type M2 and its role in tumor growth and spreading. Paper presented at the Seminars in cancer biology
- Montaldi AP, Godoy PR, Sakamoto-Hojo ET (2015) APE1/REF-1 down-regulation enhances the cytotoxic effects of temozolomide in a resistant glioblastoma cell line. *Mutation Research/Genetic Toxicology and Environmental Mutagenesis* 793:19–29
- Mukherjee J, Phillips JJ, Zheng S, Wiencke J, Ronen SM, Pieper RO (2013) Pyruvate kinase M2 expression, but not pyruvate kinase activity, is up-regulated in a grade-specific manner in human glioma. *PLoS One* 8:e57610
- Nath S, Roychoudhury S, Kling MJ, Song H, Biswas P, Shukla A, Band H, Joshi S, Bhakat KK (2017) The extracellular role of DNA damage repair protein APE1 in regulation of IL-6 expression. *Cell Signal* 39:18–31
- Redaelli A, Magrassi R, Bonassi S, Abbondandolo A, Frosina G (1998) AP endonuclease activity in humans: development of a simple assay and analysis of ten normal individuals. *Teratog Carcinog Mutagen* 18:17–26
- Sabarinathan D, Mahalakshmi P, Vanisree AJ (2011) Naringenin, a flavanone inhibits the proliferation of cerebrally implanted C6 glioma cells in rats. *Chem Biol Interact* 189:26–36
- Schleicher SM, Thotala DK, Linkous AG, Hu R, Leahy KM, Yazlovitskaya EM, Hallahan DE (2011) Autotaxin and LPA receptors represent potential molecular targets for the radiosensitization of murine glioma through effects on tumor vasculature. *PLoS One* 6:e22182
- Shida D, Kitayama J, Yamaguchi H, Okaji Y, Tsuno NH, Watanabe T, Takuwa Y, Nagawa H (2003) Lysophosphatidic acid (LPA) enhances the metastatic potential of human colon carcinoma DLD1 cells through LPA1. *Cancer Res* 63:1706–1711
- Silber JR, Bobola MS, Blank A, Schoeler KD, Haroldson PD, Huynh MB, Kolstoe DD (2002) The apurinic/aprimidinic endonuclease activity of Ape1/ref-1 contributes to human glioma cell resistance to alkylating agents and is elevated by oxidative stress. *Clin Cancer Res* 8:3008–3018
- Singh S, Englander EW (2012) Nuclear depletion of apurinic/aprimidinic endonuclease 1 (Ape1/ref-1) is an indicator of energy disruption in neurons. *Free Radic Biol Med* 53:1782–1790
- Sosa V, Moline T, Somoza R, Paciucci R, Kondoh H, Leonart ME (2013) Oxidative stress and cancer: an overview. *Ageing Res Rev* 12:376–390
- Tamada, M., Suematsu, M., & Saya, H. (2012). Pyruvate kinase M2: multiple faces for conferring benefits on cancer cells: American Association for Cancer Research
- Tell G, Quadrifoglio F, Tiribelli C, Kelley MR (2009) The many functions of APE1/ref-1: not only a DNA repair enzyme. *Antioxid Redox Signal* 11:601–619
- Tell G, Fantini D, Quadrifoglio F (2010) Understanding different functions of mammalian AP endonuclease (APE1) as a promising tool for cancer treatment. *Cell Mol Life Sci* 67:3589–3608
- Umez-Goto M, Kishi Y, Taira A, Hama K, Dohmae N, Takio K, Yamori T, Mills GB, Inoue K, Aoki J (2002) Autotaxin has lysophospholipase D activity leading to tumor cell growth and motility by lysophosphatidic acid production. *J Cell Biol* 158:227–233
- Valko M, Rhodes C, Moncol J, Izakovic M, Mazur M (2006) Free radicals, metals and antioxidants in oxidative stress-induced cancer. *Chem Biol Interact* 160:1–40
- Wrensch M, Minn Y, Chew T, Bondy M, Berger MS (2002) Epidemiology of primary brain tumors: current concepts and review of the literature. *Neuro-Oncology* 4:278–299
- Wu J-M, Xu Y, Skill NJ, Sheng H, Zhao Z, Yu M, Saxena R, Maluccio MA (2010) Research Autotaxin expression and its connection with the TNF-alpha-NF-kB axis in human hepatocellular carcinoma. *Mol Cancer* 9:1–14
- Xiangyuan Y, Xiaomin N (2017) Desuccinylation of pyruvate kinase M2 by SIRT5 contributes to antioxidant response and tumor growth. *Oncotarget* 8:6984
- Yamada T, Sato K, Komachi M, Malchinkhuu E, Tobo M, Kimura T, Kuwabara A, Yanagita Y, Ikeya T, Tanahashi Y (2004) Lysophosphatidic acid (LPA) in malignant ascites stimulates motility of human pancreatic cancer cells through LPA1. *J Biol Chem* 279:6595–6605
- Yang W, Lu Z (2013) Nuclear PKM2 regulates the Warburg effect. *Cell Cycle* 12:3343–3347